COMPUTATIONAL FLOW PREDICTION
IN CYCLONE CHAMBERS

Georgios Haralampou Vatistas

A Thesis

in

The Faculty

of

Engineering

Presented in Partial Fulfillment of the
Requirements for the Degree of Master
of Engineering at Concordia University
Montreal, Quebec

July 1980

ABSTRACT

COMPUTATIONAL FLOW PREDICTION

IN CYCLONE CHAMBERS

Georgios Haralampou Vatistas

A theoretical prediction procedure has been developed to analyze the physical processes taking place in cyclone chambers. For this, the transient two-dimensional (2-D) Los Alamos SOLA solution algorithm has been extended to include the effects of the tangential velocity component for the flowfield which is assumed to be axisymmetric. The numerical solution procedure utilizes a simplified form of the Marker and Cell solution technique focussing attention on the steady-state case. A rapidly convergent algorithm is achieved by applying the method developed by the Imperial College group for treating the outlet boundary condition. Predictions for a cyclone chamber with a single-or a multi-set of tangential inlets show that a useful characterization of their flowfield is now becoming available.

ACKNOWLEDGEMENT

The author expresses his appreciation to his supervisor, Professor C.K. Kwok for his guidance and valuable advices throughout the course of this investigation.

Sincere thanks go to friend and teacher Professor D.G. Lilley of Oklahoma State University who provided him with solid foundations with which to successfully complete the present work.

Thanks are due to Professor P.M. Lee for his very constructive suggestions.

The author is deeply grateful to his parents for their patience and encouragement.

The present investigation was partially supported by the National Research Council of Canada under Grant No. A7435.

TABLE OF CONTENTS

LIST OF FIGURES

NOMENCLATURE

D	chamber's diameter, m, (ft)
d	diameter of the outlet port, m, (ft)
Div	divergence
g	body acceleration, m/s^2, (ft/s^2)
h	height of the inlet port, m, (ft)
L	chamber's length, m, (ft)
o	order of magnitude
P	ratio of pressure to density, $(N/m^2)/kg$, $(lb/ft^2/lbm)$
Q	volume flowrate, m^3/s, (ft^3/s)
R	radius m, (ft), Reynolds number
S	inlet swirl strength, $S = W_{IN}/U_{IN}$
t	time, s
U	velocity component in x direction, m/s, (ft/s)
V	velocity component in y direction, m/s, (ft/s)
W	velocity component in θ direction, m/s, (ft/s)
x, y, θ	radial, axial and tangential directions
Z	radial station
z	distance of the radial station from the base plate m, (ft)
α	upstream - differencing constant
δ	boundary layer thickness, m, (ft)
Δt	time increment, s
$\Delta x, \Delta y$	radial and axial distances between two neighboring mesh points, m, (ft)
ΔP	pressure increment, $N/m^2/kg$, $(lbf/ft^2/lbm)$

ε	pressure - iteration convergence criterion
ν	kinematic viscosity, m^2/sec, (ft^2/sec)
ϕ	generalized property
ω	over relaxation factor

SUBSCRIPTS

e	effective properties
IN	properties at the inlet port.
i,j	mesh-point indexes
L	properties based on the chamber's length
o	distance of the velocity component in i,j cell from the datum
OUT	properties at the outlet port

SUPERSCRIPTS

n	time level t
—	average quantities

CHAPTER 1

INTRODUCTION

The main problem of energy recovery from solid wastes centers upon the design of efficient combustion chambers, which must be such, as to cause retention of fuel particles until they are completely burnt. The combustion chambers for solid fuel, which approach the desired characteristics, are cyclone furnaces with vortex action to segregate heavy and light particles.

Prior knowledge of the aerodynamic flow pattern within such chambers is necessary for a furnace designer to select an optimum configuration for an efficient, pollution-free furnace design. However, the extreme complexity of the natural mechanism involved renders the problem of setting up a mathematical model for the flow pattern more difficult. In general, the difficulties involved are:

a) The inability of the mathematical equations to truly portray the flow phenomenon in great precision.

b) The failure of the existing mathematical methods to give an exact solution to the set of partial differential equations.

Recent development of high-speed electronic computing machines provides the means to solve these equations using numerical methods with a high degree of accuracy. The present work may be considered as a first step towards solving multi-dimensional cyclone chamber problems with complex boundary conditions.

1.1 THE PHENOMENON

Vortex chambers are used extensively in furnace engineering and several other high temperature applications. In general, they have a cylindrical configuration with a central axis outlet and circumferential inlets. Entry of fluid through the tangential inlets produces a swirling motion inside the vortex chamber. The inlets may be arranged near the outlet end of the chamber or at the opposite end or both. The advantages and main characteristics of the cyclone process are primarily due to the particular pattern of the flow-field produced. It in turn, depends on a number of design parameters, including the diameter and length of the chamber, size of the outlet, size and location of the inlets, and also the velocity and supply rates through the inlets.

The objective of the present work is to predict numerically the vortex flow-field within a chamber taking into consideration the geometric configuration and inlet flow conditions.

1.2 PREVIOUS WORK

The subject of confined vortex flows found in Cyclone Chambers has received considerable attention in the past twenty years owing to the great potential of such a system.

In a comprehensive survey article, Syred et al[1], reviewed the combustion problems of low calorific-value gases in various types of cyclone combustors. The early experimental work of Kalisheovshevshii and Gachev[2] was directed towards the detailed investigation of the velocity and temperature distributions for a horizontal cyclone furnace. Later, Baluev and Troyankin[3] performed an outstanding experimental study about the cold aerodynamic structure of gas flow in a vertical chamber. Continuing their investigations, the same authors[4] further studied the effects of several design parameters on the aerodynamics of the same experimental model. An extensive research about the turbulent flow structure of such flows was carried out by Ustimenko and Bukhman[5]. Troyankin and Baluev[6] further extended the investigations of their model to include the effects of the chamber's resistance on the flow and the furnace's aerodynamic efficiency. Finally, an article by Tager et al[7] revealed the relationship between the chamber's outlet diameter to its overall flow pattern. The above experimental work, was accomplished using stationary models consisting of tangential inlet(s), either near the top or near the bottom plate of the chamber. The furnaces used were positioned either horizontally or vertically.

In the area of theoretical investigation, Wormley[8] provided an analytical foundation to the study of vortex flow in short cylindrical chambers. Most of the subsequent theoretical work is based upon Wormley's original analysis. A semi-analytical investigation for a liquid in a swirl chamber was conducted by Koval and Michailov[9].

Most of the theoretical models attempted so far used either short or long chambers. This is due to the fact that certain approximations can be made allowing investigators to reduce the Navier-Stokes equation in a form amenable to analytical treatment. The fact that a cyclone furnace does not belong to either of the two, above-mentioned categories leads to a much more complex flow-field. Furthermore, the associated equations can only be solved utilizing numerical methods.

1.3 METHOD OF APPROACH

Consideration is given to the development of a primitive-variable, finite-difference solution procedure for an axisymmetric swirling flow in cyclone chambers. The present work is developed from a previous concept concerning the solution of a 2-D non-swirling flow using the Los Alamos[10] technique for treating the transient case, and the Imperial College[11] method for treating the steady-state case directly.

The transient two-dimensional Los Alamos SOLA prediction technique has been extended to include the computation of an axisymmetric swirling flow. Attention is directed towards the steady-state form of the flow-field. The outlet conditions have been modified using the Imperial College method for rapid convergence. The principal interest is centered upon keeping the algorithm simple, with the appreciation that any user-oriented sophistications can be added as required to the basic algorithm[12,13].

Useful computational results on the aerodynamics of the cyclone-chamber performance for several input conditions and configurations indicate that a tool for the furnace designer to predict cyclone flow pattern is now becoming possible.

CHAPTER 2

THEORETICAL MODEL

Consideration is given to the development of a finite-difference solution procedure for 2-D swirling flows in cyclone chambers. Chapter 2 and 3 of the thesis present the Marker and Cell (MAC) simulation and solution techniques, focussing attention directly on the primitive pressure and velocity variables. A 2-D version is described in Reference 10, upon which the present work is based. An Eulerian finite-difference formulation is developed using pressure and velocity as the main dependent variables. In addition, the U and V velocity components are positioned between the nodes where pressure and tangential velocity variables are stored. At each time step, the time-marched expressions for U, V and W are substituted into the continuity equation for each cell, and the guess-and-correct iterative process on pressure and velocity corrections are performed until continuity is sufficiently well satisfied.

2.1 THE PROBLEM

A schematic and physical dimensions of the mathematical model used to simulate the processes is illustrated in figure 1. The cyclone chamber studied has a cylindrical shape with a constant cross-sectional area. Fluid, of uniform velocity, is admitted into the chamber through swirling vanes which regulate the relative strength of the tangential (W_{IN}), and radial (U_{IN}) velocity components. Inlets are located along the upper and lower periphery of the chamber's wall. The outlet is located centrally on the top plate and a special restriction is arranged to prevent flow escaping from the top inlet directly to the outlet port.

The theoretical model is designed to correctly simulate the flow with respect to its geometric configuration, physical properties of the fluid and boundary conditions.

2.2 GOVERNING EQUATIONS

In order to arrive at a model amenable to mathematical treatment, some simplifications are necessary. The fluid is assumed to be incompressible with constant kinematic viscosity ν. The flow is also assumed to be axisymmetrical, therefore, all the dependant variables U, V, W and P become only functions of x, y and t. Commencing with the 3-D equation of fluid motion,[14] and taking into consideration the axisymmetry of the problem, the governing equations are then given as:

Continuity,

$$\frac{\partial U}{\partial x} + \frac{U}{x} + \frac{\partial V}{\partial y} = 0 \qquad (2.2.1)$$

U-momentum

$$\frac{\partial U}{\partial t} + U\frac{\partial U}{\partial x} + V\frac{\partial U}{\partial y} - \frac{W^2}{x} = -\frac{\partial P}{\partial x} + \nu\left(\frac{\partial^2 U}{\partial x^2} + \frac{1}{x}\frac{\partial U}{\partial x} + \frac{\partial^2 U}{\partial y^2} - \frac{U}{x^2}\right) + g_x \qquad (2.2.2)$$

V-momentum

$$\frac{\partial V}{\partial t} + U\frac{\partial V}{\partial x} + V\frac{\partial V}{\partial y} = -\frac{\partial P}{\partial y} + \nu\left(\frac{\partial^2 V}{\partial x^2} + \frac{1}{x}\frac{\partial V}{\partial x} + \frac{\partial^2 V}{\partial y^2}\right) + g_y \qquad (2.2.3)$$

W-momentum

$$\frac{\partial W}{\partial t} + U\frac{\partial W}{\partial x} + \frac{UW}{x} + V\frac{\partial W}{\partial y} = \nu\left(\frac{\partial^2 W}{\partial x^2} + \frac{1}{x}\frac{\partial W}{\partial x} + \frac{\partial^2 W}{\partial y^2} - \frac{W}{x^2}\right) + g_\theta \qquad (2.2.4)$$

The coordinate system used is shown in figure 2. To transform the above equation into a conservative form (i.e. the divergence of momentum flux), for the convective members the following procedure is applied.

The convective portion of the U-momentum equation is,

$$U\frac{\partial U}{\partial x} - \frac{W^2}{x} + V\frac{\partial U}{\partial y} \qquad (2.2.2a)$$

By rearranging, the above equation becomes

$$U\frac{\partial U}{\partial x} + U\frac{\partial U}{\partial x} - U\frac{\partial U}{\partial x} + V\frac{\partial U}{\partial y} + U\frac{\partial V}{\partial y} - U\frac{\partial V}{\partial y} - \frac{W^2}{x}$$

or

$$\frac{\partial(U^2)}{\partial x} - U\frac{\partial U}{\partial x} + \frac{\partial}{\partial y}(UV) - U\frac{\partial V}{\partial y} - \frac{W^2}{x}$$

which can be reduced to,

$$\frac{\partial}{\partial x}(U^2) + \frac{\partial}{\partial y}(UV) - U\left(\frac{\partial U}{\partial x} + \frac{\partial V}{\partial y}\right) - \frac{W^2}{x} \qquad (2.2.2b)$$

Substituting continuity equation of (2.2.1) into expression (2.2.2b), one obtains,

$$\frac{\partial}{\partial x}(U^2) + \frac{\partial}{\partial y}(UV) + \frac{U^2-W^2}{x}$$

and the U- momentum equation can be expressed as,

$$\frac{\partial U}{\partial t} + \frac{\partial}{\partial x}(U^2) + \frac{\partial}{\partial y}(UV) + \left(\frac{U^2-W^2}{x}\right) = -\frac{\partial P}{\partial x} + \nu\left(\frac{\partial^2 U}{\partial x^2} + \frac{1}{x}\frac{\partial U}{\partial x} + \frac{\partial^2 U}{\partial y^2} - \frac{U}{x^2}\right) + g_x \qquad (2.2.5)$$

If the same technique is applied to the other V and W momentum equations, their conservative form may be written as[15,16].

V - momentum

$$\frac{\partial V}{\partial t} + \frac{\partial}{\partial x}(UV) + \frac{\partial}{\partial y}(V^2) + \frac{UV}{x} = -\frac{\partial P}{\partial y} + \nu\left(\frac{\partial^2 V}{\partial x^2} + \frac{1}{x}\frac{\partial V}{\partial x} + \frac{\partial^2 V}{\partial y^2}\right) + g_y \qquad (2.2.6)$$

W - momentum

$$\frac{\partial W}{\partial t} + \frac{\partial}{\partial x}(WU) + \frac{\partial}{\partial y}(WV) + 2\frac{UW}{x} = \nu\left(\frac{\partial^2 W}{\partial x^2} + \frac{1}{x}\frac{\partial W}{\partial x} + \frac{\partial^2 W}{\partial y^2} - \frac{W}{x^2}\right) + g_\theta \qquad (2.2.7)$$

2.3 THE FLOW REGION AND GRID SYSTEM

Figure 3 shows how the flow region on a meridional plane is divided into rectangular cells. This flow region is surrounded by a layer of fictitious cells on all sides to incorporate the boundary conditions (B Cs).

A cell is magnified in figure 4, which shows the location of each variable, P, U, V and W. The pressure and tangential velocity are located at the center of the cell, and the radial and axial velocities positioned on the right (vertical) and top (horizontal) sides, respectively. Thus normal velocities (to the wall) lie directly on the physical boundaries of the domain, which is defined as the region enclosed by the boundaries, while the tangential velocities and pressures are placed at half cell intervals. This arrangement greatly simplifies the application of boundary conditions.

CHAPTER 3

SOLUTION PROCEDURE

3.1 THE FINITE DIFFERENCE EQUATIONS

Mathematically, the governing equations are parabolic (in time) and a marching solution procedure is adapted.

Starting from initial field values throughout the domain, a time-march process is used to advance the flow-field towards the final steady-state. The numerical method employed uses Forward-Time, Centered-Space (FTCS) difference scheme[10]. The usual one-sided, first time derivatives and centered, second space derivatives are used in representing these equations. However, special techniques in computational fluid dynamics in the representation of the convective terms are required. A certain amount of upstream differencing is given to these terms (the donor cell approach) to remove the unconditional instability of the resulting algorithm in case that a very small viscosity is used.

The following are the difference equations representing the conservation of momentum in x,y and θ directions:

$$
\begin{aligned}
U_{i,j} &= U_{i,j}^{n} + \Delta t \left\{ \frac{1}{\Delta x} (P_{i,j}^{n} - P_{i+1,j}^{n}) + g_x - FUX - FUY - FUC + VISX \right\} \\
V_{i,j} &= V_{i,j}^{n} + \Delta t \left\{ \frac{1}{\Delta y} (P_{i,j}^{n} - P_{i,j+1}^{n}) + g_y - FVX - FVY - FVC + VISY \right\} \qquad (3.1.1) \\
W_{i,j} &= W_{i,j}^{n} - \Delta t \left\{ FWX + FWY + FWC - VISZ \right\}
\end{aligned}
$$

where, FUX, FUY, FUC, FVX, FVY, FVC, FWX, FWY and FWC are the convective fluxes while VISX, VISY and VISZ are the viscous fluxes (see Appendix A). Superscripts n and (blank) are used to denote values of time-level t and $t + \Delta t$, respectively.

If the convective terms of these equations are to be evaluated with the central difference approximation and the viscosity is very small, instability will result. In order to alleviate this without resorting to a less accurate algorithm, the upstream differencing scheme must be applied. That is, if ϕ is a general property and if the donor cell approach is used, see figure 5, then the following conditions must be satisfied:

$$\frac{\partial\phi}{\partial x} = \begin{cases} \left.\frac{\partial\phi}{\partial x}\right|_{x_0} - \frac{\alpha\Delta x}{4} \cdot \left.\frac{\partial^2\phi}{\partial x^2}\right|_{x_0} + o(\Delta x^2) & \text{if } \phi_{i,j} \geq \frac{\phi_{i+1,j} + \phi_{i-1,j}}{2} \\ \left.\frac{\partial\phi}{\partial x}\right|_{x_0} + \frac{\alpha\Delta x}{4} \left.\frac{\partial^2\phi}{\partial x^2}\right|_{x_0} + o(\Delta x^2) & \text{if } \phi_{i,j} < \frac{\phi_{i+1,j} + \phi_{i-1,j}}{2} \end{cases} \tag{3.1:2}$$

The coefficient α is a constant taking a value between zero and one, and so giving the desired amount of upstream differencing in the convection terms[10]. A value of zero gives merely central differencing code which is second-order accurate in Δx, however numerical instability problems arise. A value of one gives full upstream differencing which, though introducing errors, is stable, provided the other stability criteria are satisfied.

Therefore,

$$FUX = \left.\frac{\partial U^2}{\partial x}\right|_{x_o} - \frac{\alpha\Delta x}{4} \left.\frac{\partial^2 U^2}{\partial x^2}\right|_{x_o} + o\,(\Delta x^2)$$

or,

$$FUX = \frac{(U_{i+1,j} + U_{i,j})^2 - (U_{i-1,j} + U_{i,j})^2}{4\Delta x}$$

$$- \frac{\alpha\Delta x}{4} \left(\frac{U_{i-1,j}^2 - 2U_{i,j}^2 + U_{i+1,j}^2}{\Delta x^2} \right) + o\,(\Delta x^2)$$

$$= \frac{1}{4\Delta x} \Big[(U_{i+1,j} + U_{i,j})^2 - (U_{i-1,j} + U_{i,j})^2$$

$$- \alpha \Big\{ (U_{i-1,j} + U_{i,j})\,(U_{i-1,j} - U_{i,j}) - (U_{i,j} + U_{i+1,j})$$

$$(U_{i,j} - U_{i+1,j}) \Big\} \Big] + o\,(\Delta x^2) \qquad (3.1.3)$$

To assure that,

$$FUX = \begin{cases} \left. FUX \right|_{x_o - \frac{\alpha\Delta x}{4}} & \text{if} \quad U_{i,j} \geq \dfrac{U_{i+1,j} + U_{i-1,j}}{2} \\[2ex] \left. FUX \right|_{x_o + \frac{\alpha\Delta x}{4}} & \text{if} \quad U_{i,j} < \dfrac{U_{i+1,j} + U_{i-1,j}}{2} \end{cases}$$

equation (3.1.3) becomes:

$$FUX = \frac{1}{4\Delta x} \Big[(U_{i+1,j} + U_{i,j})^2 + \alpha \left| U_{i,j} + U_{i+1,j} \right| (U_{i,j} - U_{i+1,j})$$

$$- (U_{i-1,j} + U_{i,j})^2 - \alpha \left| U_{i-1,j} + U_{i,j} \right| (U_{i-1,j} - U_{i,j}) \Big]$$

$$+ o\,(\Delta x^2) \qquad (3.1.4)$$

Following the same reasoning and to assure that:

$$FUY = \begin{cases} FUY\Big|_{y_0 - \frac{\alpha\Delta y}{4}} & \text{if} \quad U_{i,j} \geq \frac{U_{i+1,j} + U_{i-1,j}}{2} \\ FUY\Big|_{y_0 + \frac{\alpha\Delta y}{4}} & \text{if} \quad U_{i,j} < \frac{U_{i+1,j} + U_{i-1,j}}{2} \end{cases}$$

then,

$$FUY = \frac{1}{4\Delta y} \Big[(V_{i,j} + V_{i+1,j})(U_{i,j} + U_{i,j+1}) + \alpha | V_{i,j} + V_{i+1,j} | (U_{i,j} - U_{i,j+1}) - (V_{i,j-1} + V_{i+1,j-1}) (U_{i,j-1} + U_{i,j}) - \alpha | V_{i,j-1} + V_{i+1,j-1} | (U_{i,j-1} - U_{i,j}) \Big] + o\,(\Delta y^2) \qquad (3.1.5)$$

The same technique is applied in order to approximate the rest of the convective terms of the equation (3.1.1) and they are defined in Appendix A.

3.2 PRESSURE CORRECTION EQUATIONS

Although equation (3.1.1) enables one forward time-step to be accomplished, the newly calculated velocities will not, in general, satisfy the continuity requirement, as expressed in central finite difference form

$$\frac{1}{\Delta x} (U_{i,j} - U_{i-1,j}) + \frac{1}{\Delta y} (V_{i,j} - V_{i,j-1}) + \frac{1}{2\Delta x (i-1.5)} (U_{i,j} + U_{i-1,j}) = 0 \qquad (3.2.1)$$

Terms here are evaluated at time-level $t + \Delta t$.

This incompressibility constraint is imposed by iteratively adjusting the cell pressure. That is, if the divergence, Div, of a cell is positive (the left side of equation (3.2.1) is positive), there is a net mass-flow from that cell. This is corrected by reducing the cell pressure. On the other hand, if the divergence is negative, an increase in cell pressure is necessary.

When the cell pressure changes from P to P + ΔP the velocity components on the four faces of the cell change. The amount changed is expressed as,[10]

$$
\begin{aligned}
U_{i,j} &= U_{i,j}\ (OLD) + \frac{\Delta t \Delta P}{\Delta x} \\
U_{i-1,j} &= U_{i-1,j}\ (OLD) - \frac{\Delta t \Delta P}{\Delta x} \\
V_{i,j} &= V_{i,j}\ (OLD) + \frac{\Delta t \Delta P}{\Delta y} \\
V_{i,j-1} &= V_{i,j-1}\ (OLD) - \frac{\Delta t \Delta P}{\Delta y}
\end{aligned}
\qquad (3.2.2)
$$

Where (OLD) means previous level of iteration. Substituting equation (3.2.2) into equation (3.2.1) one obtains,

$$
\begin{aligned}
&\frac{1}{\Delta x}\left(U_{i,j}(OLD) - U_{i-1,j}(OLD)\right) + \frac{1}{\Delta y}\left(V_{i,j}(OLD) - V_{i,j-1}(OLD)\right) \\
&+ \frac{1}{2\Delta x(i-1.5)}\left(U_{i,j}(OLD) + U_{i-1,j}(OLD)\right) = \\
&\qquad - 2\left(\frac{\Delta t \Delta P}{\Delta x^2} + \frac{\Delta t \Delta P}{\Delta y^2}\right)
\end{aligned}
\qquad (3.2.3)
$$

Since the left side equals the divergence of the previous iteration level (OLD), equation (3.2.3) becomes,

$$\text{Div (OLD)} = - 2\left(\frac{\Delta t \Delta P}{\Delta x^2} + \frac{\Delta t \Delta P}{\Delta y^2}\right)$$

Then the amount of correction to the pressure is:

$$\Delta P = - \text{Div (OLD)} / \left(2\Delta t\ (1/\Delta x^2 + 1/\Delta y^2)\right) \qquad (3.3.4)$$

Pressure update iteration continues until the divergence of all the cells are less than some prescribed small positive quantity ε. An over-relaxation factor ω near 1.8 often is applied[10] to equation (3.2.4)

$$\Delta P = -\omega \, \text{Div (OLD)} \, / \, (2\Delta t \, (1/\Delta x^2 + 1/\Delta y^2))$$

in order to speed up the convergence of the pressure-iteration process.

3.3. BOUNDARY CONDITIONS

In the previous sections the finite difference equations (FDE's) approximating the governing partial differential equations (PDE's), are set up and solved by way of a time-march process applied to cells within the flow domain of interest. A single layer of fictitious cells are placed around the flow region thus utilizing the value on the boundary.

Rigid wall boundaries are defined in such a way as to coincide with cell boundaries. For interior normal velocity calculations, zero normal values on the rigid wall are assumed. Interior tangential (to the wall) velocity calculations use the fictitious values which are placed in the surrounding layer of complementary computational cells. Specification of these is after each time-step and after each sweep of the cells during the pressure correction iteration. The tangential velocity component has a vanishing gradient across a no-slip boundary, and this is achieved by setting the external values of the velocity equal to the negative of their immediate associated interior values, see figure 6. The free-slip boundary is met by setting the external tangential velocity value equal to their immediate associated interior values, as shown in figure 7.

Some care has to be taken in the selection of either no-slip or free-slip boundary conditions to assure a realistic picture of the flow-field. For an actual fluid, no-slip condition implies the development of a boundary layer. The velocity increases from zero value at the rigid wall to the free stream value some distance from it. The boundary layer thickness may be large or small in comparison to the cell's dimension. As it can be seen from figure 8, a small value of boundary layer thickness δ relative to the cell's dimension, gives a bad approximation to the velocity profile and imposes an artificially large drag on the field. An estimation of the magnitude of the boundary layer thickness can be made utilizing the elementary boundary layer theory. According to simple theory[17] on laminar flow, the boundary layer thickness is expressed as

$$\delta \sim \frac{L}{\sqrt{R_L}}$$

where:

L = length of the chamber

R_L = $L\bar{V}/\nu$

$\bar{V}$ = average axial velocity within the chamber

If the displacement thickness δ^* is expressed as

$$\delta^* = \frac{3}{4}\,\delta$$

and if,

$\delta^* < \frac{1}{4}\,\Delta y$ then the boundary layer is considered to be "thin".

if, $\delta^* \geq \frac{1}{4}\,\Delta y$ then the boundary layer is "thick".

Therefore, for a coarse grid, free-slip boundary conditions are appropriate for the tangential velocities. On the other hand, with a fine grid over the flow-field, or with a fine grid in the wall's neighborhood, no-slip boundary conditions are needed.

Specifications of normal velocities at an outflow boundary often pose a problem, as it can have a detrimental upstream influence. One might merely impose the normal gradient of continuative condition and set these values to their immediate upstream values as shown in figure 9. When primary interest is being focused on the final steady-state, a constant value may be added to each such extrapolated value. This will result in a more rapid convergence. This constant value is chosen so as to make the total outlet flux equal to the total inlet flux, thus satisfying the condition of continuity. Outlet boundary specification is imposed, only each time-step as computed via equation (3.2.1) and not after each pass through the mesh during the pressure iteration.

On the axis of symmetry, the usual zero normal velocity and free-slip axial velocity specifications are applicable; the swirl velocity is given a definite zero value via no-slip condition as shown in Fig.10.

Inlet boundary conditions are satisfied by imposing a zero gradient on the radial and swirl velocity components, while the axial velocity components are forced to zero on the fictitious exterior cells as shown in figure 11.

3.4 STABILITY CONSIDERATIONS

Attempts to solve PDE's numerically using a finite difference method are not always successful. The reason is that the solution to the FDE's may be dominated from a monotonic or oscillatory error growth which will in no way resemble the solution expected from the original PDE's. To avoid this difficulty, stability considerations and appropriate restrictions have to be applied on the algorithm. Since a non-linear theoretical stability treatment is essentially non existent for the present problem, the following simple heuristic method along with numerical experimentation was found to give very reasonable stability criteria.

The derived FDE's link only those cells which have common boundaries. A fluid particle that propagates more than one cell for each time step cannot be monitored by the FDE's. The algorithms, thereby, fail to be stable. To assure stability, the fluid particle must not be allowed to cross more than one cell for each time step. The worst cases that can exist in a flow-field are in those regions where the velocities assume their maximum values. Thus the following two inequalities must be satisfied,

$$\Delta x > |U_{MAX}\, \Delta t| \quad \text{and} \quad \Delta y > |V_{MAX}\, \Delta t|$$

Solving, for Δt, both inequalities,

$$\Delta t \leq \frac{\Delta x}{|U_{MAX}|} \quad \text{and} \quad \Delta t \leq \frac{\Delta y}{|V_{MAX}|}$$

or,

$$\Delta t < \min \left\{ \frac{\Delta x}{|U_{MAX}|} , \frac{\Delta y}{|V_{MAX}|} \right\} \tag{3.4.1}$$

Assume that the PDE for the general property ϕ has the form:

$$\frac{\partial \phi}{\partial t} + U \frac{\partial \phi}{\partial x} + V \frac{\partial \phi}{\partial y} = - \frac{\partial P}{\partial x} + \nu \left(\frac{\partial^2 \phi}{\partial x^2} + \frac{\partial^2 \phi}{\partial y^2} \right) \tag{3.4.2}$$

Assume further that U and V are constants, then the FDE becomes,

$$\frac{\phi_{i,j} - \phi^n_{i,j}}{\Delta t} = - U \frac{\phi^n_{i+1,j} - \phi^n_{i-1,j}}{2\Delta x} - V \frac{\phi^n_{i,j+1} - \phi^n_{i,j-1}}{2\Delta y}$$

$$- \frac{P^n_{i+1,j} - P^n_{i,j}}{\Delta x} + \nu \left(\frac{\phi^n_{i-1,j} - 2\phi^n_{i,j} + \phi^n_{i+1,j}}{\Delta x^2} \right.$$

$$\left. + \frac{\phi^n_{i,j+1} - 2\phi^n_{i,j} + \phi^2_{i,j-1}}{\Delta y^2} \right)$$

or,

$$\phi_{i,j} = \Delta t \nu \left(\frac{\phi^n_{i-1,j} + \phi^n_{i+1,j}}{\Delta x^2} + \frac{\phi^n_{i,j-1} + \phi^n_{i,j+1}}{\Delta y^2} \right) - \frac{\left(P^n_{i+1,j} - P^n_{i,j}\right)}{\Delta x} \Delta t$$

$$- \frac{\Delta t U}{2\Delta x} \left(\phi^n_{i+1,j} - \phi^n_{i-1,j} \right) - \frac{\Delta t V}{2\Delta y} \left(\phi^n_{i,j+1} - \phi^n_{i,j-1} \right)$$

$$+ \left[1 - 2\Delta t \nu \left(\frac{1}{\Delta x^2} + \frac{1}{\Delta y^2} \right) \right] \phi^n_{i,j}$$

For stability according to Reference 18,

$$1 - 2\Delta t \nu \left(\frac{1}{\Delta x^2} + \frac{1}{\Delta y^2} \right) > 0$$

therefore,

$$\nu \Delta t < \frac{1}{2} \left(\frac{\Delta x^2 \, \Delta y^2}{\Delta x^2 + \Delta y^2} \right) \qquad (3.4.3)$$

Consider the equation

$$\frac{\partial \phi}{\partial t} + U \frac{\partial \phi}{\partial x} = \nu \frac{\partial^2 \phi}{\partial x^2} \qquad (3.4.4)$$

where U is constant .

Expansion in Taylor's series about the point$(i\Delta x, n\Delta t)$ gives the donor cell equation .

$$\frac{\partial \phi}{\partial t} + \frac{\Delta t}{2} \frac{\partial^2 \phi}{\partial t^2} + U \frac{\partial \phi}{\partial x} = \nu \frac{\partial^2 \phi}{\partial x^2} + \frac{\alpha |U| \Delta x}{2} \frac{\partial^2 \phi}{\partial x^2} + o(\Delta x^2, \Delta t^2) \qquad (3.4.5)$$

Taking the time derivative of equation (3.4.4) we have,

$$\frac{\partial^2 \phi}{\partial t^2} = - U \frac{\partial^2 \phi}{\partial t \partial x} + \nu \frac{\partial^3 \phi}{\partial t \partial x^2}$$

$$= - U \frac{\partial}{\partial x} \left(-U \frac{\partial \phi}{\partial x} + \nu \frac{\partial^2 \phi}{\partial x^2}\right) + \nu \frac{\partial^2}{\partial x^2} \left(-U \frac{\partial \phi}{\partial x} + \nu \frac{\partial^2 \phi}{\partial x^2}\right)$$

Neglecting terms higher than three

$$\frac{\partial^2\phi}{\partial t^2} = U^2 \frac{\partial^2\phi}{\partial x^2} \qquad (3.4.6)$$

Substituting equation (3.4.6) into equation (3.4.5) one obtains

$$\frac{\partial\phi}{\partial t} + U\frac{\partial\phi}{\partial x} = \left(\nu + \frac{\alpha|U|\Delta x}{2} - \frac{\Delta t U^2}{2}\right)\frac{\partial^2\phi}{\partial x^2}$$

$$+ o\,(\Delta x^2, \Delta x\Delta t, \Delta t^2) \qquad (3.4.7)$$

If we let,

$$\nu_e = \nu + \frac{\alpha|U|\Delta x}{2} - \frac{\Delta t U^2}{2}$$

Then,

$$\frac{\partial\phi}{\partial t} + U\frac{\partial\phi}{\partial x} = \nu_e \frac{\partial^2\phi}{\partial x^2} \qquad (3.4.8)$$

where ν_e is known as the "effective viscosity coefficient".

Since any diffusion coefficient "smears out" uniformly any disturbance in the general property ϕ, ν_e means that the coefficient tends to concentrate any small perturbation from a uniform ϕ distribution (this is physically impossible). Therefore, for stability,

$$\nu + \frac{\alpha|U|\Delta t}{2} - \frac{\Delta t U^2}{2} > 0$$

For high R_e, the viscosity coefficient is numerically equal to zero, then

$$\frac{\alpha|U|\Delta x}{2} - \frac{\Delta t U^2}{2} > 0$$

or,

$$\alpha > \left|\frac{U\Delta t}{\Delta x}\right| \qquad (3.4.9)$$

Therefore, equation (3.4.9) must be satisfied in order to gain stability.

The algorithm is stable for any inlet swirl strength equal or less than one, if all the mentioned restrictions are followed. For inlet swirl strength greater than one, the algorithm fails to be stable, owing to the fact that the tangential velocity component dominates the radial momentum equation. After a great deal of numerical experimentation it was concluded that for convergence, if S is greater than one, Δt must satisfy the following additional inequality:

$$\Delta t < \min \left(\frac{\Delta x}{|W_{MAX}|} , \frac{\Delta y}{|W_{MAX}|} \right) \qquad (3.4.10)$$

where W_{MAX} can be taken as approximately

$$W_{MAX} = S \quad W_{IN}$$

Therefore, to assure stability of the algorithm, all the above mentioned restrictions have to be met. A summary of the stability and convergence criteria is given as follows:

Having chosen the grid size, the time increment must be restricted in three ways, and a suitable amount of upstream differencing must be effected.

(i) Since the FDE's assume fluxes only between neighbouring cells, the fluid particles can only move through one cell in one time step. Thus for stability, Δt must be less than (typically equal to 0.25 to 0.33 times) the minimum cell transit time taken over all cells:

$$\Delta t < \min \left(\left|\frac{\Delta x}{U}\right| , \left|\frac{\Delta y}{V}\right| \right)$$

(ii) When the kinematic viscosity is non zero, momentum must not diffuse more than approximately one cell in one time step for which a linear analysis shows

$$\Delta t < \frac{1}{2\nu}\left(\frac{\Delta x^2 \Delta y^2}{\Delta x^2 + \Delta y^2}\right)$$

(iii) When S is greater than one, Δt must be

$$\Delta t < \min\left(\frac{\Delta x}{|W_{MAX}|}, \frac{\Delta y}{|W_{MAX}|}\right)$$

where $W_{MAX} = S\, W_{IN}$

(iv) When the time step is so restricted, the required amount of upstream (donor cell) differencing must be achieved by choosing a value slightly greater than (typically 1.2 to 1.5 times) the larger of the right hand side members of

$$1 > \alpha > \max\left(\left|\frac{U\Delta t}{\Delta x}\right|, \left|\frac{V\Delta t}{\Delta y}\right|\right)$$

where the maximum is taken over all cells. If α is chosen to be too large, stability is being achieved at the introduction of an unnecessarily large amount of diffusion, like truncation errors known as numerical smoothing.

3.5 COMPUTATIONAL PROCEDURE

The finite difference equations along with the boundary and initial conditions constitute the necessary elements in synthesizing an algorithm which gives solutions to the given problems. The computational procedure consists of the following steps:

(i) Set initial conditions, read necessary constants.

(ii) Update the velocity.

(iii) Set boundary conditions.

(iv) Correct the pressure of the velocity in order to satisfy cell continuity.

(v) March time one time-step and return to step (ii).

Repeat the process until steady state is achieved.

The pressure iteration procedure continues until the divergences of all the cells are less than ε. All the required listings for the computation program are given in Appendix B.

CHAPTER 4

RESULTS AND DISCUSSIONS

Two kinds of computations dealing with single-and multi-stable cyclone chambers are described. For both configurations, a computational mesh of 10 X 10 in the x- and y- directions was overlaid on the plane of interest, with a cell size of 0.0079 [0.026] and 0.0320 [0.105] m [ft.], respectively. The flow fields were marched through the required time steps to assure steady-state conditions. The computations were performed utilizing a CDC Cyber 174 computer.

4.1 SINGLE-SET INLET CYCLONE FLOW

Predictions were first made for a cyclone chamber with a single set of inlets located near the base. An inlet height 0.032 m [0.105 ft.] giving a mean inlet flow-rate of 6.748×10^{-5} m^3/sec [0.143 cfm], and an average outlet velocity of 1.280 m/sec [4.20 ft./sec] was used for most of the predictions. The chamber has an aspect ratio (L/D) equal to 2. Profiles of the velocity components were graphed for the radial stations Z_1, Z_2, Z_3 and Z_4*, as shown in figure 12.

First, the effects of the inlet swirl strength were investigated. For the inlet, a flow-rate was kept constant at 6.748×10^{-5} m^3/sec [0.143 cfm]. Three different inlet swirl strengths (S), weak (S=0.1), medium (S=0.5) and strong (S=1.0) were applied. The tangential velocity profiles for the radial station Z_3 were shown for these three different swirl strengths.

The tangential velocity component, figure 13, resembles the Rankine profile with the forced portion of the vortex occuring in the proximity of the central axis. The fluid enhances it's tangential

---

* $Z_n = \frac{Z_n}{L}$

Z_n = 0.187, 0.1437, 0.687 and 0.937 where n = 1,2,3 and 4.

velocity component while moving towards the center, and thus conserves it's angular momentum. Due to the viscosity present in the fluid, the tangential velocity does not evidently increase to infinity, as in the case of the ideal inviscid fluid flow. Instead,the velocity attains the maximum value in the neighborhodd of the center axis, and then decays to zero through a forced vortex profile. The existence of viscosity also causes the velocity to undergo a smooth vortex mode transformation, and thus manifests a dual behaviour. For large inlet swirl strength, a considerable velocity increase is observed especially close to the axis of symmetry, and an abrupt vortex transition is taking place. The variation of the tangential velocity is more moderate for a weak swirl strength, and a distinct mixed vortex region is evident.

The effects of the inlet flow-rate were also tested. Inlet velocities of 0.3048 m/sec [1.0 ft/sec], 0.6096 m/sec [2.0 ft/sec], and 0.9144 m/sec [3.0 ft/sec] giving flow rates of 6.466 x 10^{-5} m^3/sec [9.137 cfm] respectively were applied keeping the rest of the parameters constant*.

The tangential and axial velocities were graphed for the radial station Z_3.

---

*Note that in order to keep the inlet Swirl Strength ($S=W_{IN}/U_{IN}$) constant, an increase of the inlet tangential velocity must be applied.

The tangential velocities in figure 14 show that the velocity increases proportionally with the inlet flow-rate. A sharp vortex mode transformation is taking place for high flow-rate, and a smoother profile is exhibited by the velocity for low inlet ones. The maximum velocity increases proportionally to the inlet flow-rate, and it is taking place always within the inner core of the vortex. In the outer flow region of the vortex, most of the momentum is in the x and θ directions since the presence of the top plate restricts the development of the velocity in the axial direction, as indicated in figure 15. As the fluid moves towards the axis of symmetry, it begins to sense the down-stream large axial pressure gradient due to the opening in the top plate. Therefore, the momentum from the x and θ directions starts to flow in the axial direction, which is manifested with an increase in the v-velocity component in that region.

Three constant viscosity values were used; $1.858 \times 10^{-5}[2.0 \times 10^{-4}]$, 1.858×10^{-4} $[2.0 \times 10^{-3}]$ and 1.858×10^{-3} $[2.0 \times 10^{-2}]$ m^2/sec $[ft^2/sec]$ in an attempt to study the viscosity effect. Figure 16 shows that as the viscosity increases, the free vortex flow is shifted towards the region close to the wall with the limiting case for the viscosity being infinity, where there is no free vortex region. In other words, when $\nu \to \infty$, the fluid is rotating as a solid body. As fluid "thins out", the forced vortex region is shifted towards the center of the symmetry with the limiting case of the fluid of no viscosity in which there is no force vortex region. For low viscosity, the axial velocity has a maximum near the axis of the chamber and then decays towards the cylindrical wall.

Figure 17 shows the effect of viscosity on axial velocities revealing that, when the position of the axial velocity is shifting towards the wall, there is an increase in viscosity. Large viscosities diffuse any sharp change of the property, thus giving a more uniform axial velocity profile across the chamber's diameter as compared with the case of lower viscosity.

The tangential, radial and axial velocity components are presented for several radial stations, and for the same cyclone chamber arrangement, to display a picture of the aerodynamic pattern produced.

The tangential velocity at station Z_1, as shown in figure 18, exhibits similar characteristics as those previously discussed. Velocity profiles for the radial stations Z_2 and Z_3 are not presented, since their shape and magnitude are almost identical to that of station Z_1. At Z_4, which is close to the central exit, the tangential velocity profile shown in figure 19 appeared to start with a defined value near the cylindrical wall and increased in magnitude as the flow moved towards the central axis following the law of angular momentum. At a distance, $R/x = 0.675$ where the exit starts, the tangential velocity adjusts itself to the outlet protruding wall and eventually reaches the no-slip condition at the "throats". Once the flow reaches inside the exit port, the velocity again icreases from zero to a maximum value resembling that of the free vortex configuration, and then decays to zero in order to satisfy the zero tangential velocity condition at the axis of symmetry.

Careful study of axial velocity profile at various stations as shown in figure 20, figure 21, figure 22 and figure 23 indicates that as the fluid moves from the bottom plate to the central exit port, there is a gradual shift of magnitude of axial velocity towards the center of the inner core region. The radial velocity generally exhibits a much smaller magnitude in comparison to the tangential and axial velocities except in Station Z_1 near the base plate as in figure 24. As fluid moves towards the central exit, magnitude of the radial velocity as shown in figure 25 becomes negligibly small.

4.2 MULTI-SET INLET CYCLONIC FLOW

The second configuration deals with the same system as previously discussed, except that inlets of one cell are now arranged near the top and the bottom plate, see figure 26.

Figure 27 shows a computer vector graph of U and V velocity components for such configurations. Inlet velocities of U_{IN} near the top and 2 U_{IN} near the bottom plate are applied. The outlet wall protruding inwards causes the fluid to move first downwards, and after joining the fluid coming from the bottom inlet port it is directed to the outlet.

Figure 28 depicts the tangential velocity for two stations, Z_3 and Z_4, for the same chamber as well as conditions.

Figure 29 shows a computer vector graph of U and V velocity components for the above geometric arrangement, but with applied inlet velocities of 2 U_{IN} and U_{IN} near the top and bottom plate respectively. The fluid coming to the chamber from the top inlet joins the rest of the fluid further down towards the bottom plate in a manner similar to that of the previous arrangement. For this inlet condition a lower magnitude of the tangential velocity is observed across the length of the chamber (Figure 30).

Focusing attention on the tangential velocity profile of station Z_3 near the exit, figure 31 shows the influence of the degree of inlet swirl strength on the tangential velocity development.

CHAPTER 5

CONCLUSIONS

A prediction procedure for axisymmetric swirling flows in cyclone chambers has been developed. Based on the Los Alamos 2-D SOLA ideas, the transient Navier-Stokes equations of an incompressible fluid are solved via their associated finite-difference equations directly in terms of the primitive pressure-velocity variables. The technique is kept simple in order to facilitate its usage by persons with less experience in computational fluid dynamics, and boundary conditions are simple to specify. Thus, the code represents a basic tool, to which user oriented sophistications can easily be added if necessary. Computations show the flow prediction within single-and multi-set of inlets cyclone chamber, indicating that an initial attempt to solve a highly complex vortex flow problem has been successful.

REFERENCES

1. Syred, N., Dahmen, K.R., Styles, A.C. and Najim, S.A., "A Review of Combustion Problems Associated with Low Calorific Value Gases." J. Institute of Fuel, Dec. 1977, p. 195.

2. Kalishevkii, L.L. and Ganchev, B.G.,"A Study of Combustion in a Horizontal Cyclone Furnace". Thermal Engineering, Vol. 12, 1965, p. 96.

3. Baluev, E.D. ,and Troyankin, Y.V., "Study of the Aerodynamic Structure of Gas Flow in a Cyclone Chamber." Thermal Engineering, Vol. 14, 1967, p. 84.

4. Baluev, E.D. ,and Troyankin, Y.V., "The Effect of the Design Parameters on the Aerodynamics of Cyclone Chambers." Thermal Engineering, Vol. 14, 1967, p. 99.

5. Ustimenko, B.P., and Bukhman, M.A. "Turbulent Flow Structure in a Cyclone Chamber". Thermal Engineering, Vol. 15, 1968, p. 64.

6. Troyankin , Y.U., and Baluev, E.D. "The Aerodynamic Resistance and Efficiency of a Cyclone Chamber". Thermal Engineering, Vol. 16, 1969, p. 29.

7. Tager, S.A. Motin, G.I., Talumaa, R.Yu., "Influence of the Relative Diameter of the Outlet on Characteristics of Combustion of Oil in Cyclones." Thermal Engineering, Vol. 19, 1972, p.35.

8. Wormley, D.N., "An Analytical Model for Incompressible flow in Short Vortex Chambers". J. of Basic Engineering, Trans. ASME, Series D, Vol. 92, No. 2, June 1969, p. 264.

9. Koval, V.P. and Michailov, S.L. "Velocity and Pressure Distribution of Liquid in a Swirl Chamber", Thermal Engineering, Vol. 19, 1972, p. 25.

10. Hirt, C.W., Nichols, B.D., and Romero, N.C., "SOLA-A Numerical Solution Algorithm for Transient Fluid Flows". Report LA-5852, Los Alamos Scientific Laboratory, Los Alamos, N. Mexico, 1975.

11. Gosman, A.D. and Pun, W.H., Lecture Notes for course entitled, Calculation of Recirculating Flows, Report HTS/74/2, Dept., of Mechanical Engineering, Imperial College, London, 1974.

12. Lilley, D.G., Rhode, D.L., and Vatistas, G.H., "Computational Fluid Dynamics, A Basic Approach", a report presented at the first AIAA Central Oklahoma Mini-Symposium held in The Univeristy of Oklahoma, February 24, 1979.

13. Vatistas, G.H., Lilley, D.G., and Rhode , D.L., "Fully Three-Dimensional flowfields, A Simplified Approach", a report presented at the First AIAA Central Oklahoma Mini-Symposium held in The University of Oklahoma, February 24, 1979.

14. Schlichting, H., "Boundary-"Layer Theory", 6th edition McGraw-Hill, New York, 1968.

15. Lilley, D.G., and Vatistas, G.H., "Flow Prediction in Cyclone Chambers", a report presented at Combustion Institute Canadian Section Meeting held in Ottawa, Canada, May 4 / 5, 1978.

16. Kwok, C.K., and Vatistas, G.H., " A Computer Study of Multi-Stable Cyclone Furnace Aerodynamics", paper accepted for presentation at the ASME Century II International Computer

Technology Conference taking place in San Francisco, August 10 - 23, 1980.

17. Nichols, B.D., and Hirt, C.W., "Improved free Surface Boundary Conditions for Numerical Incompressible-flow Calculations", Journal of Computational Physics, Academic Press, New York, Vol. 8, No. 3, Dec. 1971, p. 434.

18. Murman, M.E., "Computational Methods for Inviscid Transonic Flows in Imbedded Shock Waves". AGARD LECTURE SERIES NO. 48, May, 1972.

19. Hirt, W.C., "A Simple Scheme for Second Order Accuracy in Marker-And-Cell Codes." A Los Alamos Scientific Laboratory Report, Los Alamos, N. Mexico, 3 April 1976.

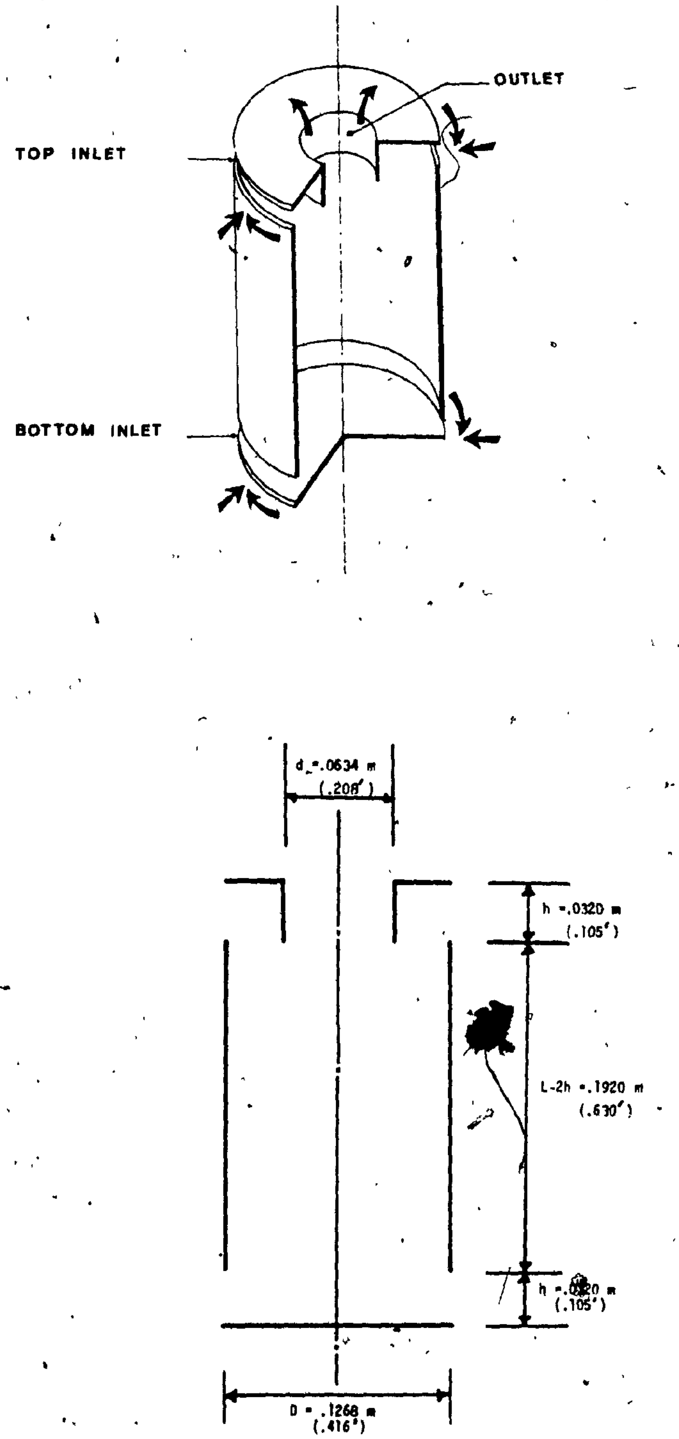

Figure 1: Cyclone Chamber Schematic and Physical Dimensions

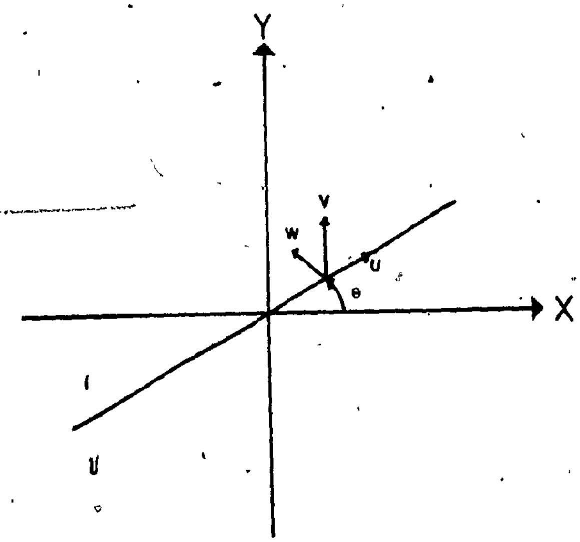

Figure 2: Coordinate System

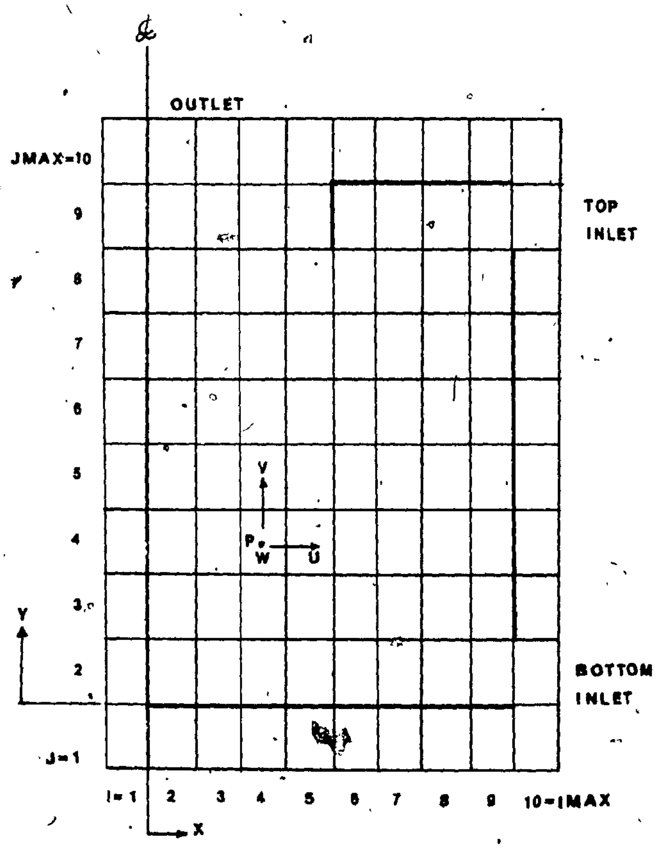

Figure 3: General Mesh Arrangement

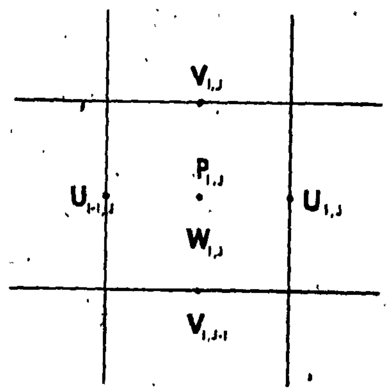

Figure 4: Arrangement of Finite Difference Variables in a Typical Cell.

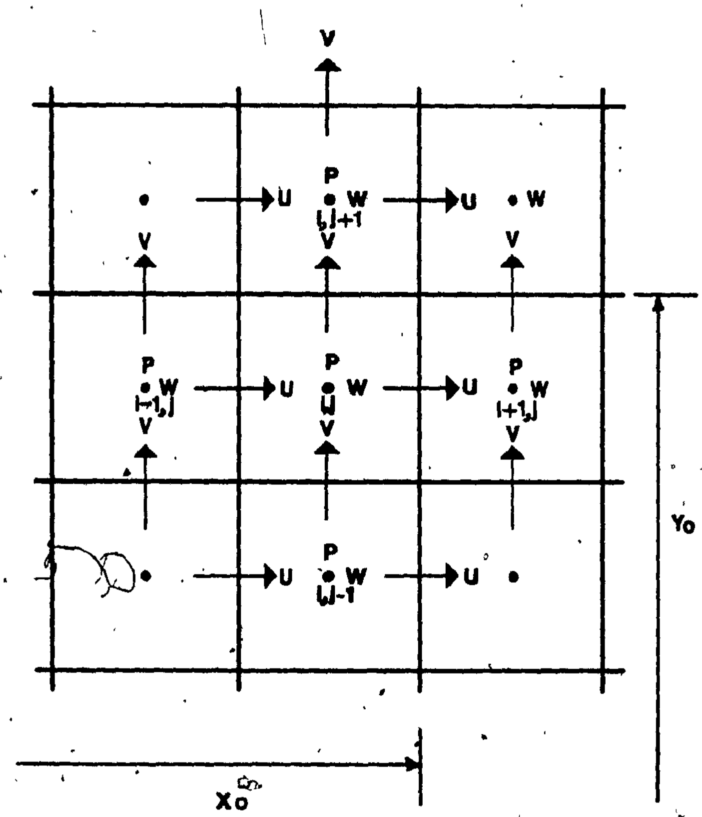

Figure 5: Typical Marker and Cell Mesh Structure

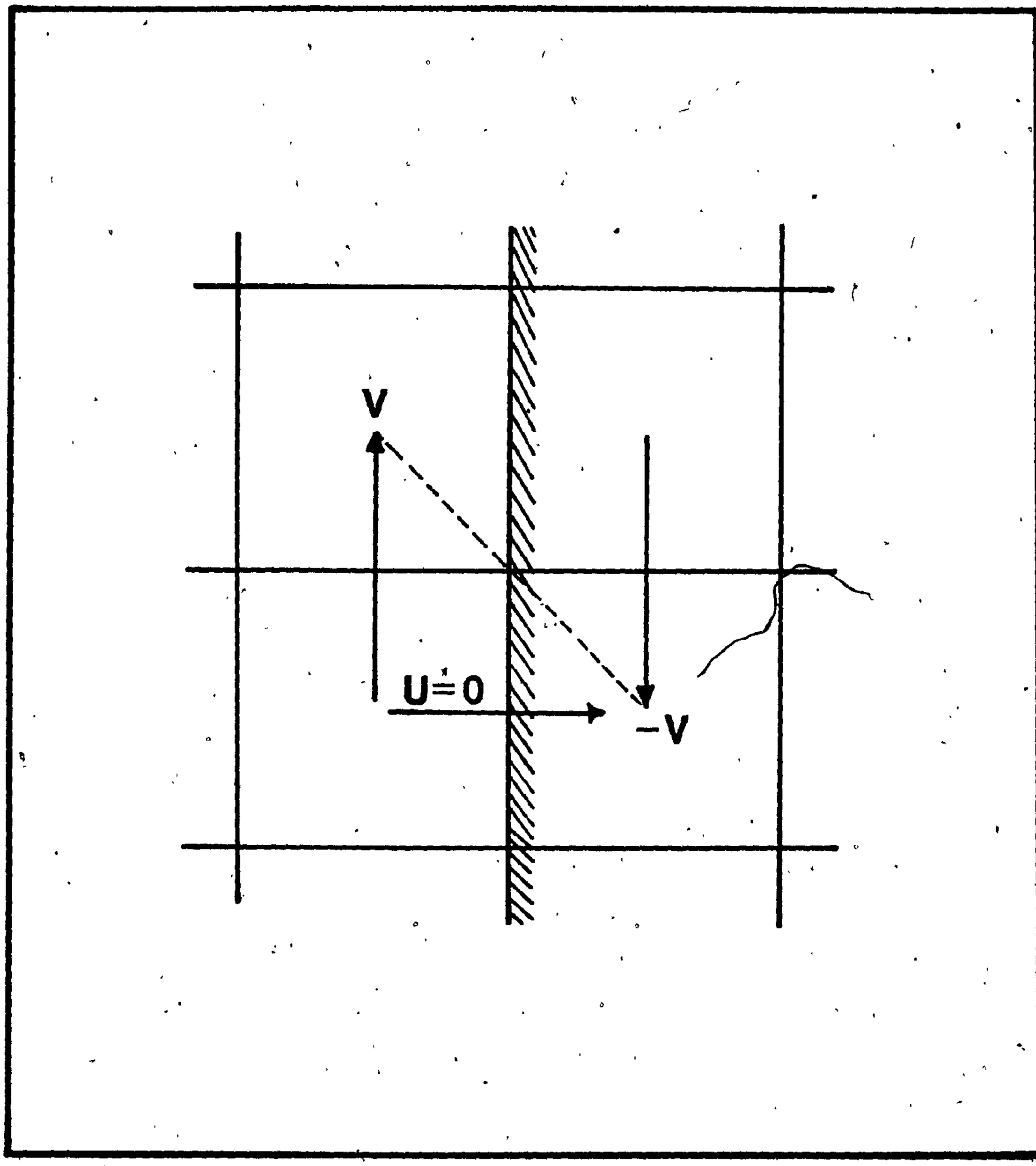

Figure 6: Rigid, No-Slip Boundary Conditions.

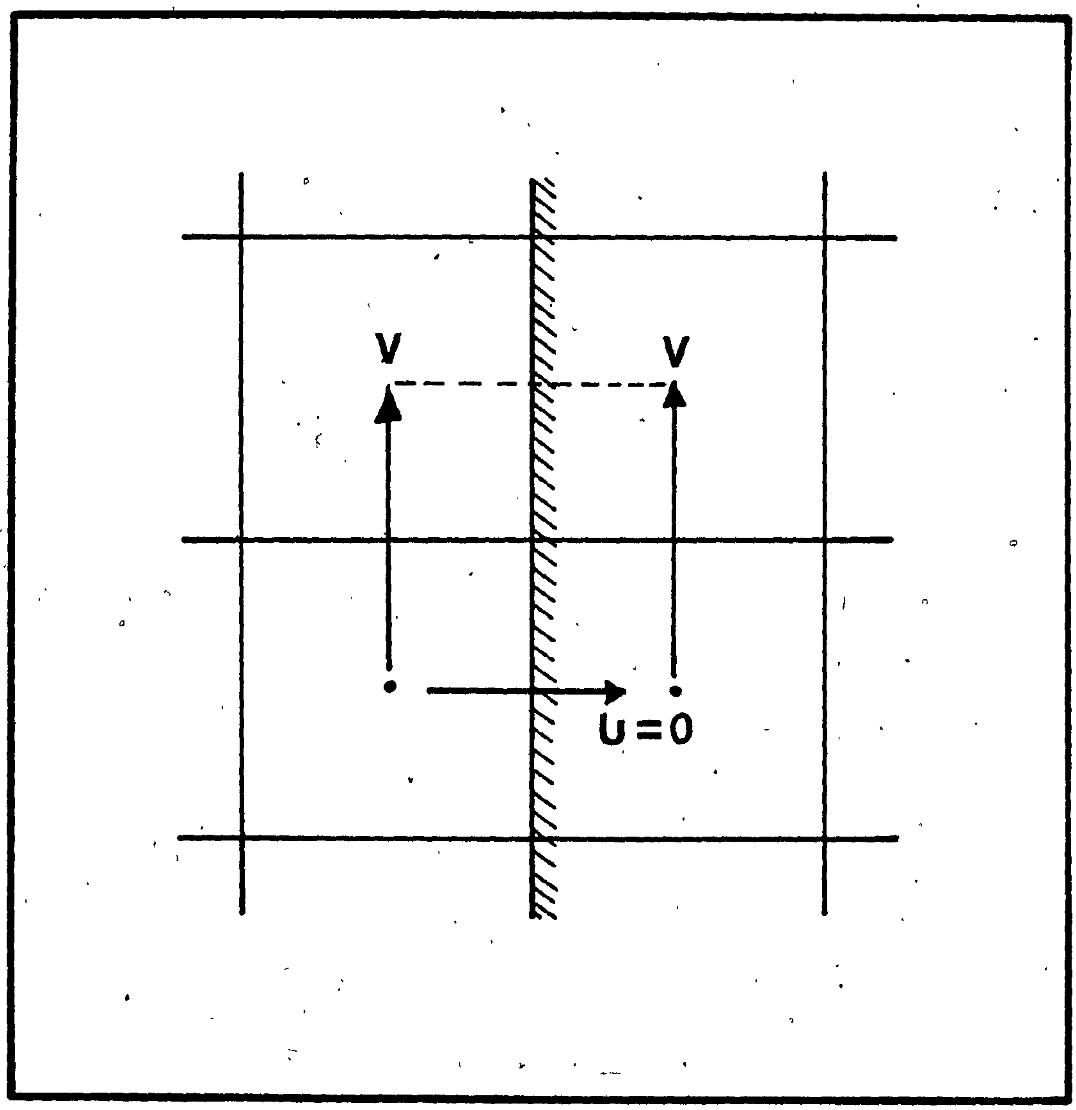

Figure 7: Rigid, Free-Slip Boundary Conditions.

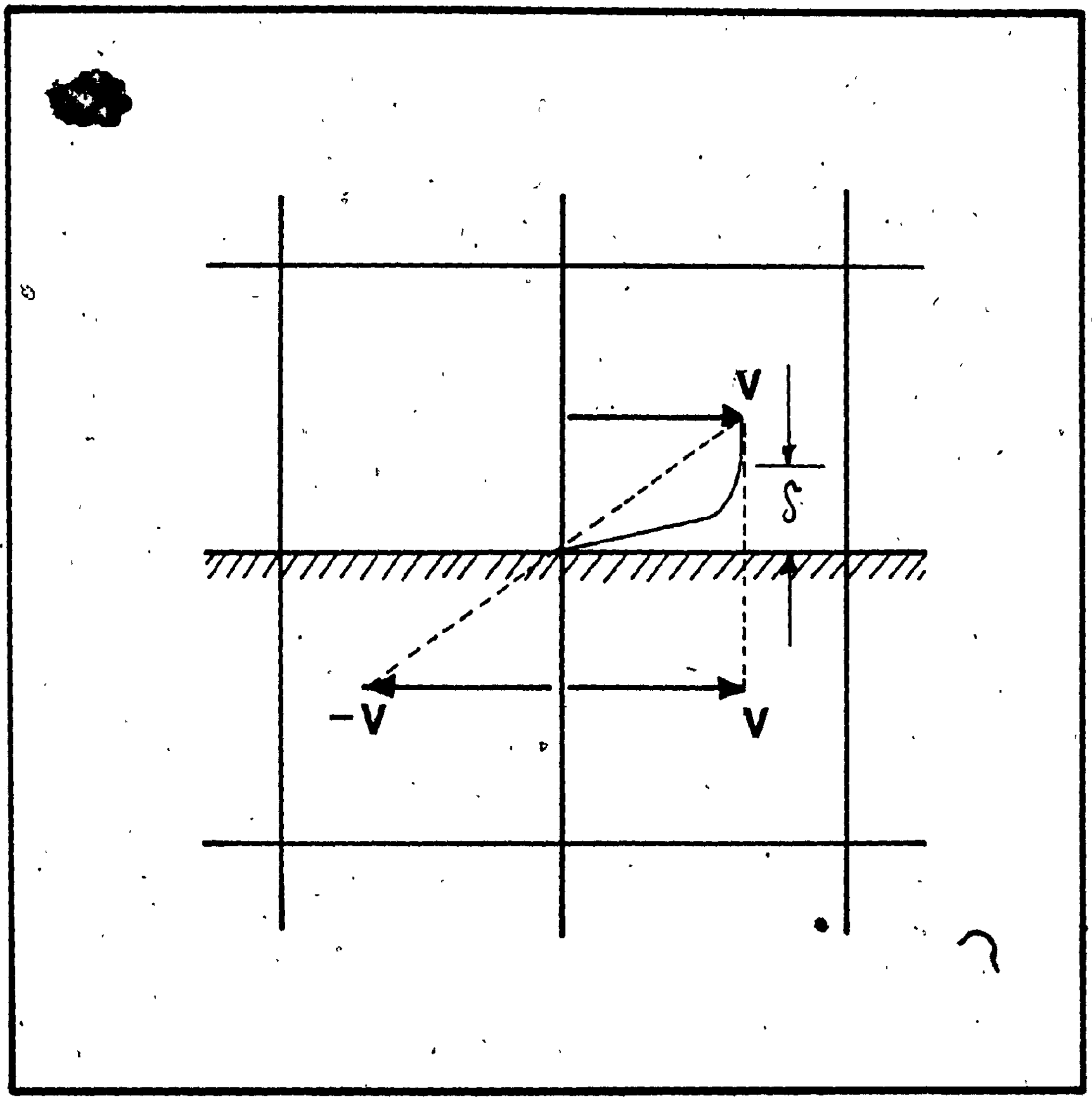

Figure 8: Numerical And Actual Velocity Distribution for Flows With Large Reynold's Numbers.[17]

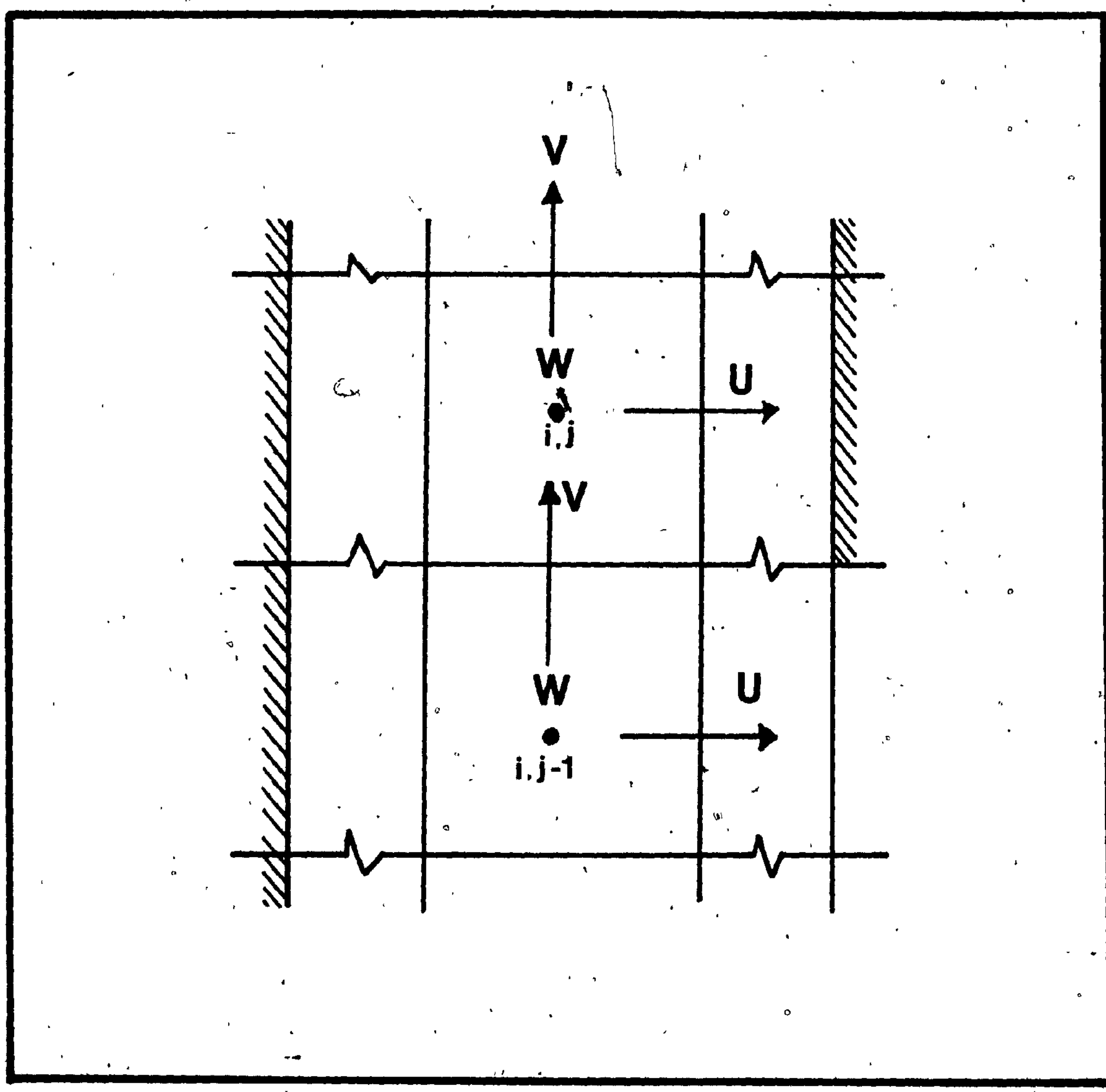

Figure 9: Continuative Outflow

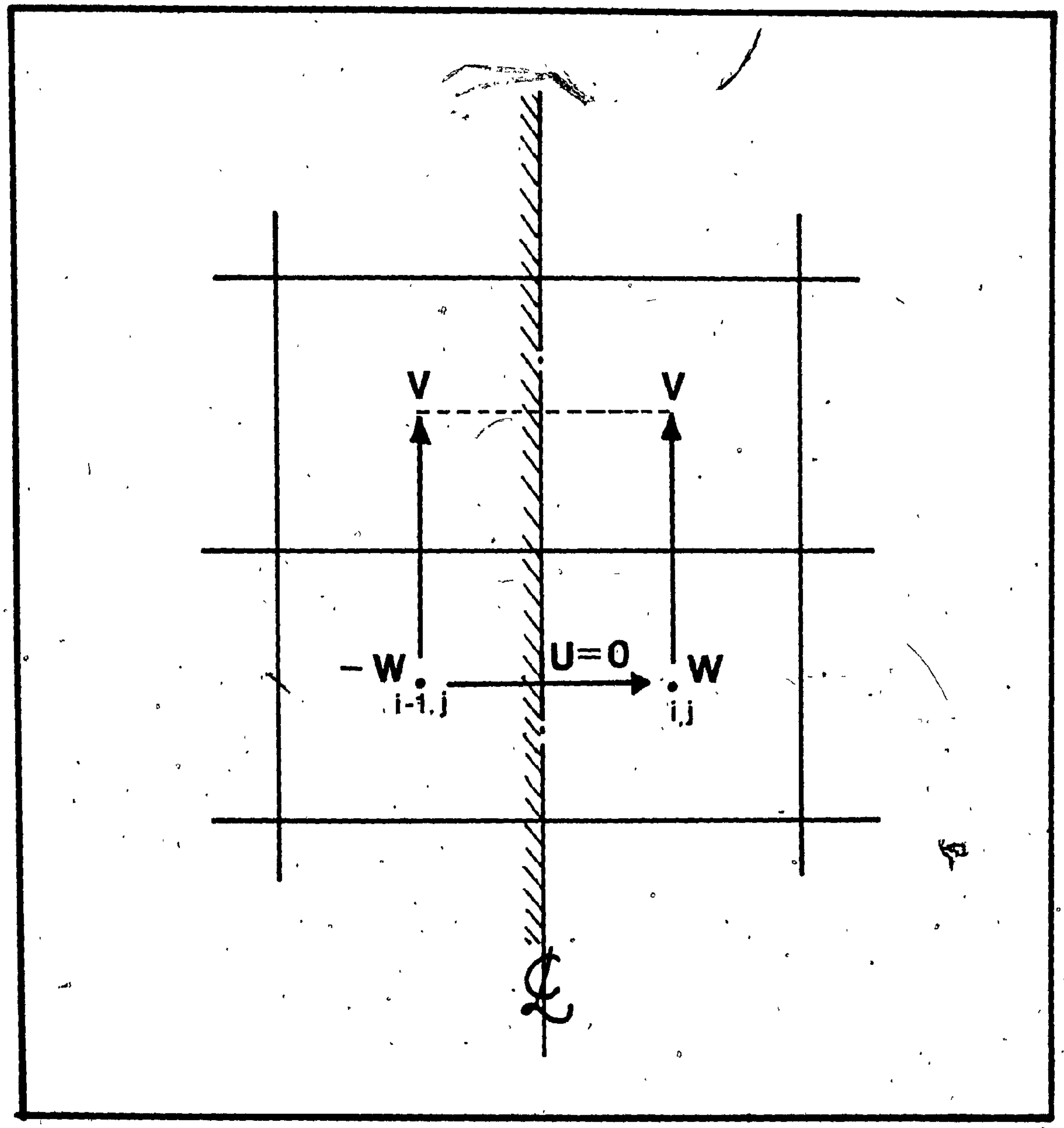

Figure 10: Boundary Condition On The Axis of Symmetry

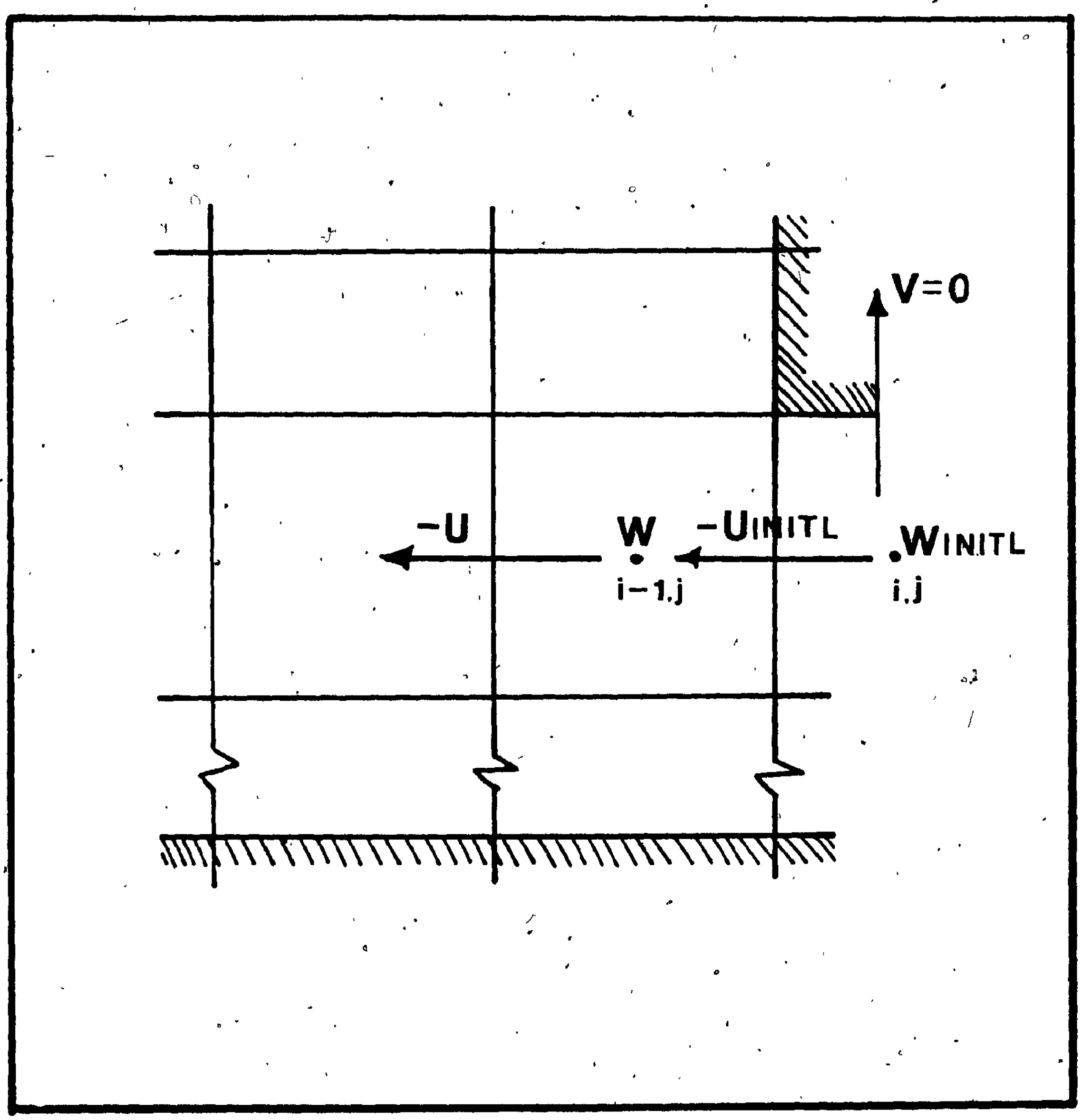

Figure 11: Inlet Boundary Conditions

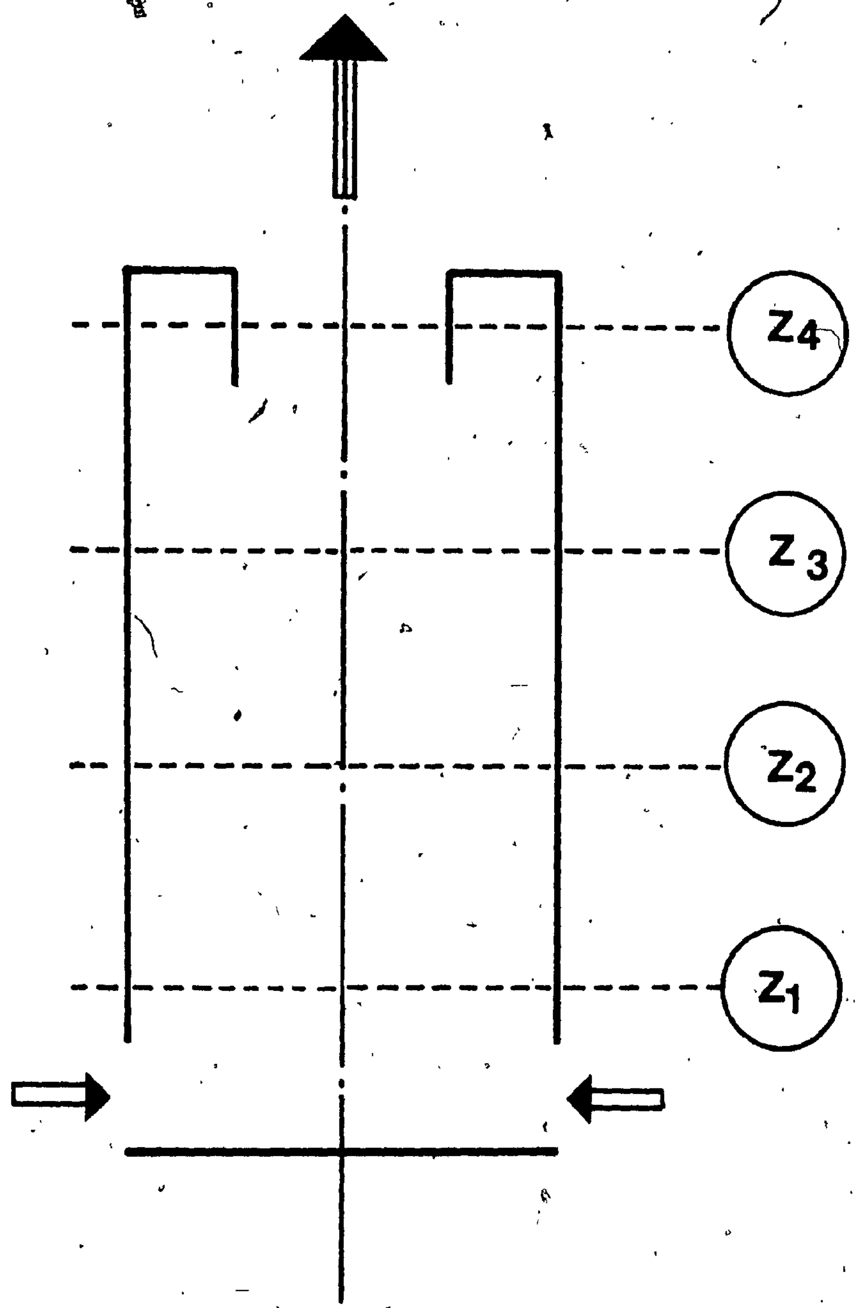

Figure 12: Schematic of a Single-Set of Inlets Cyclone Chamber and Arrangement of the Radial Stations.

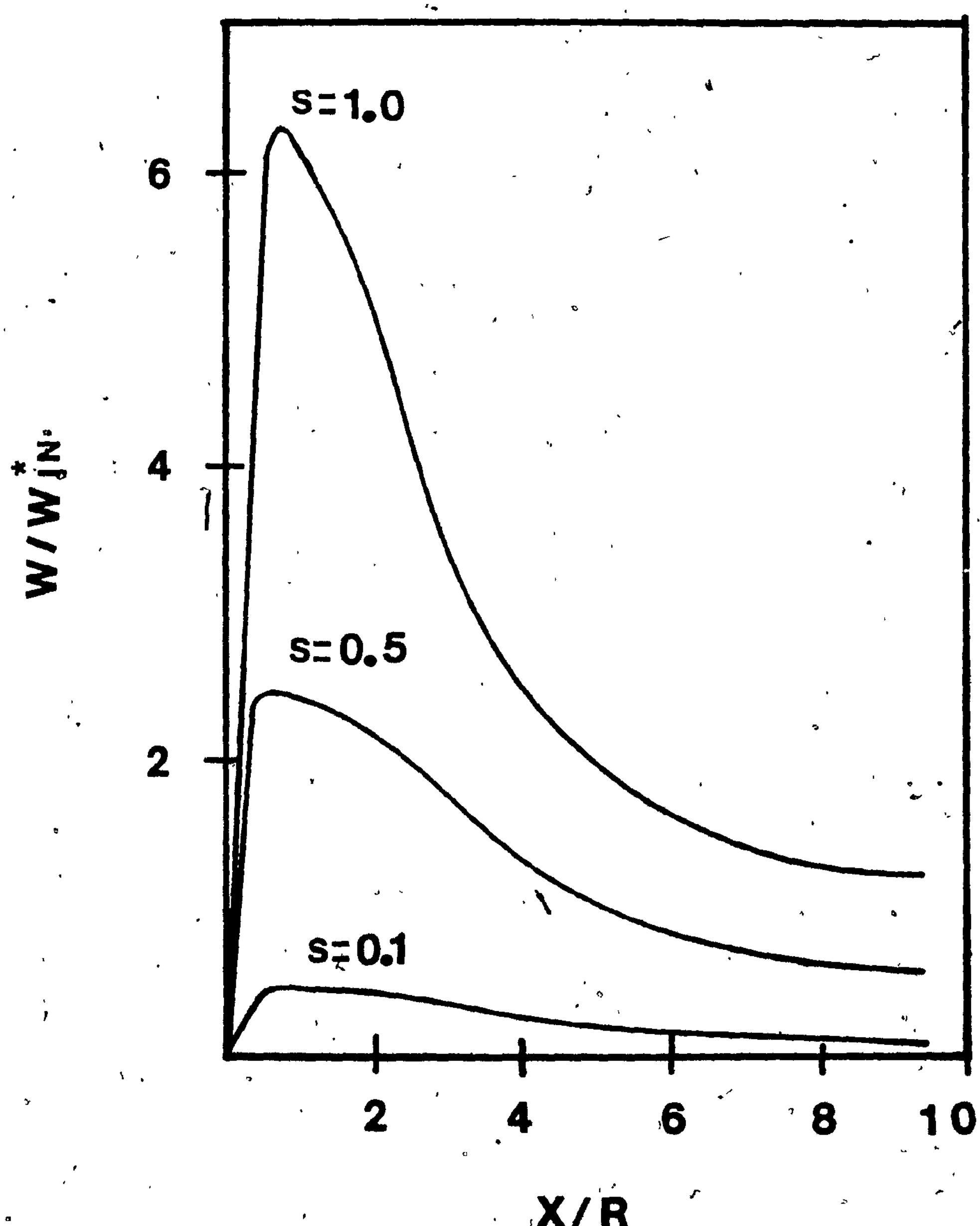

Figure 13: Tangential Velocity Profiles at Radial Station Z_3 for Different Inlet-Swirl Strengths.

* W*IN = .317 m/s (1.04 ft/s)

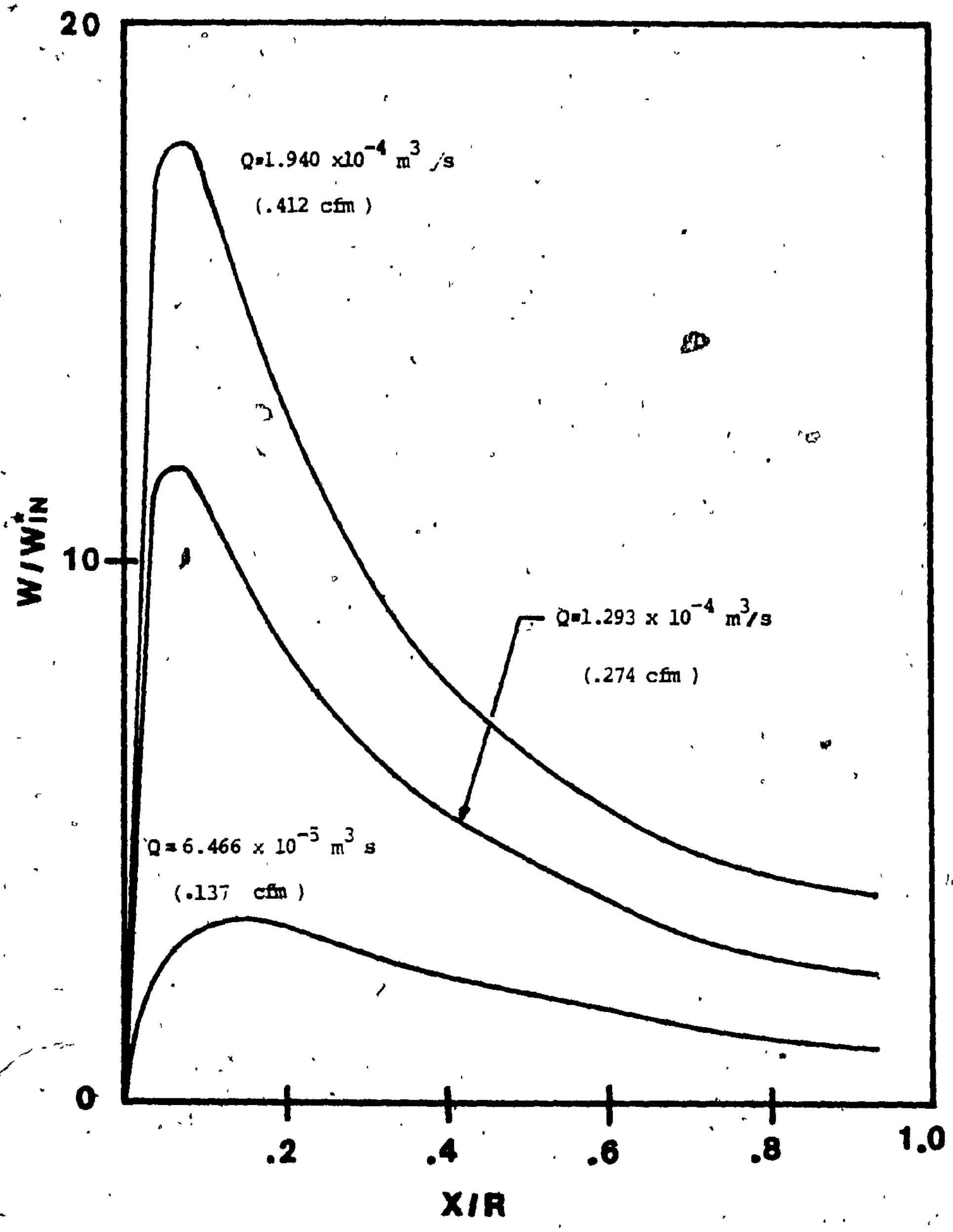

Figure 14: Tangential Velocity Profiles at Radial Station Z_3 for Different Inlet Flowrates

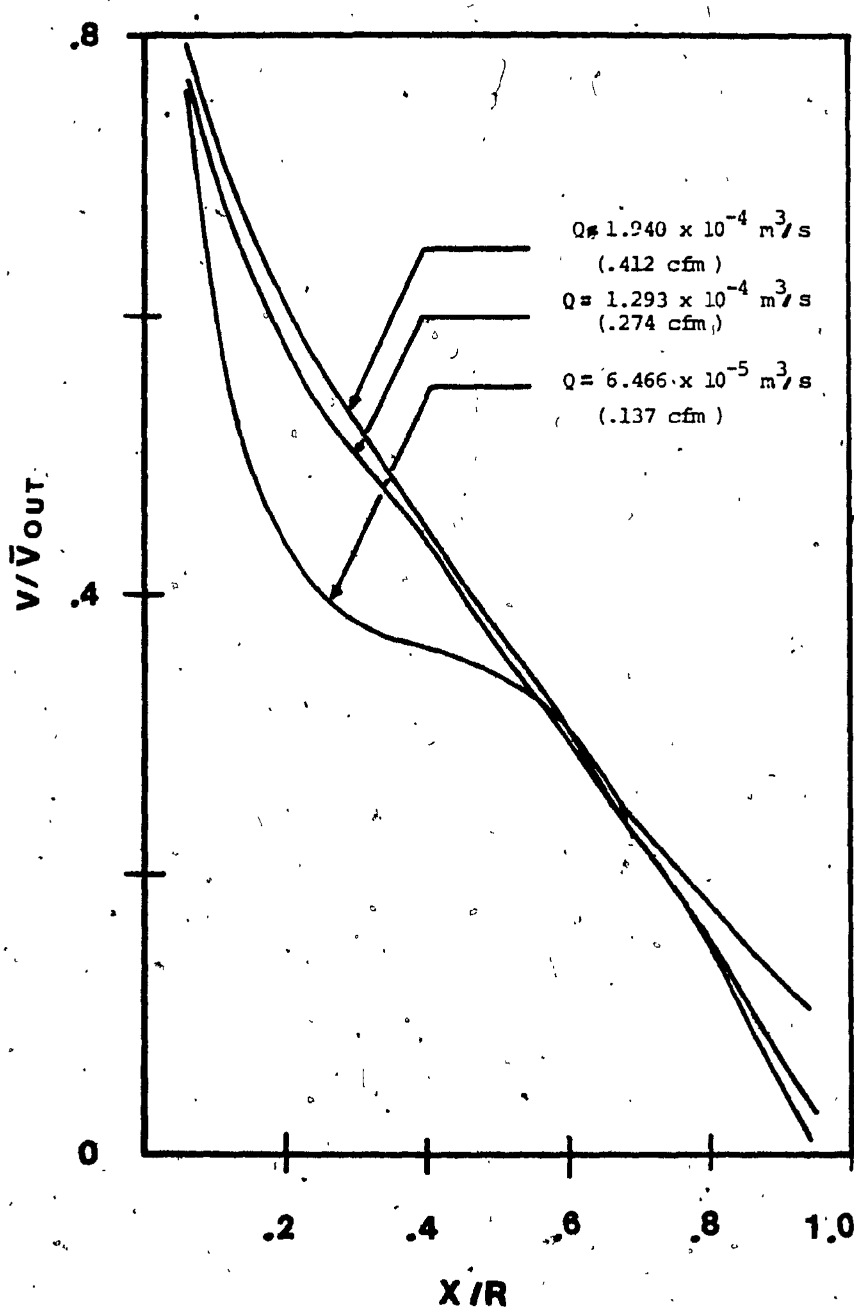

Figure 15: Axial Velocity Profiles at Radial Station Z_3 for Different Inlet Flowrates.

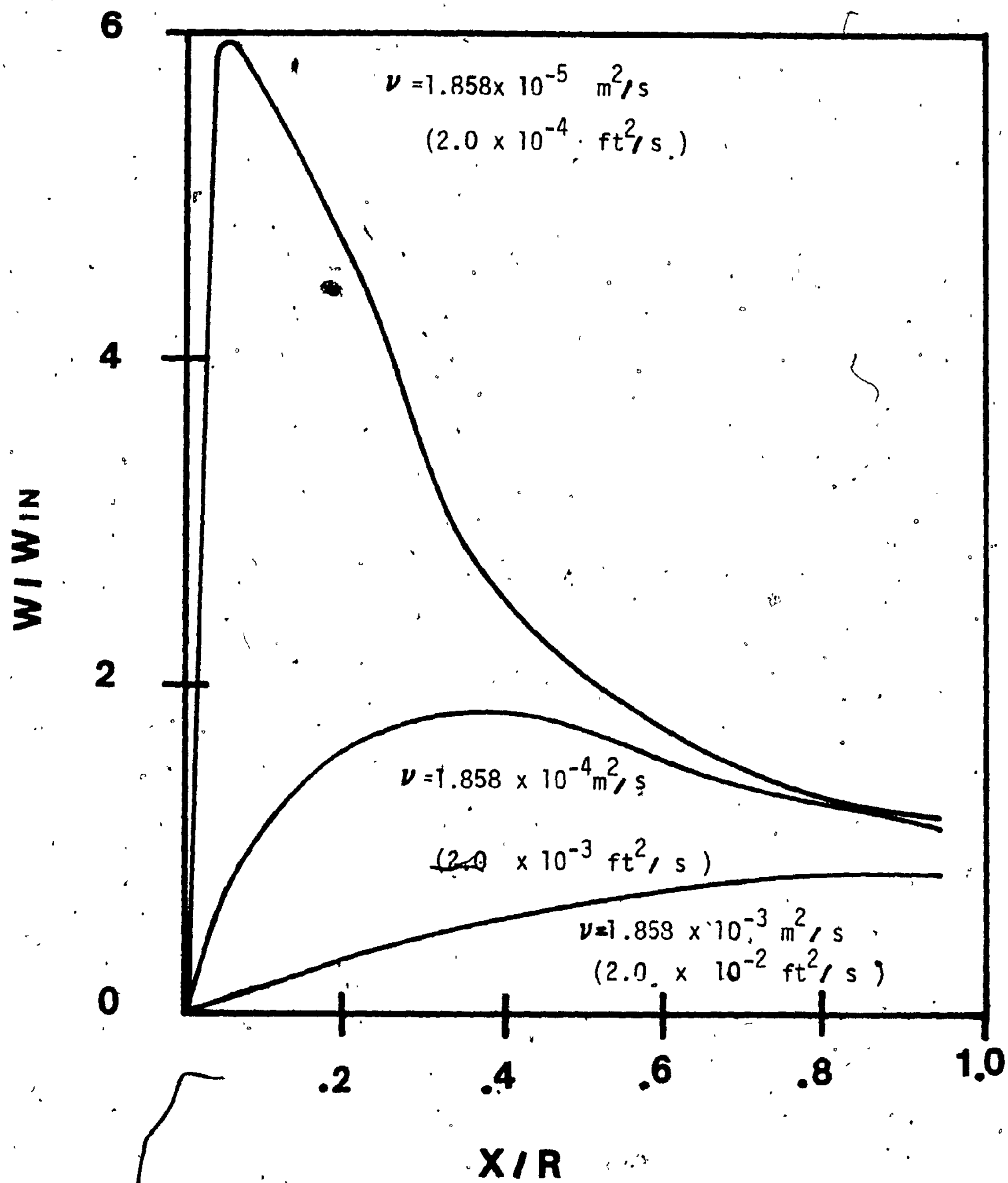

Figure 16: Tangential Velocity Profiles at Radial Station Z_3 for Different Constant Viscosities.

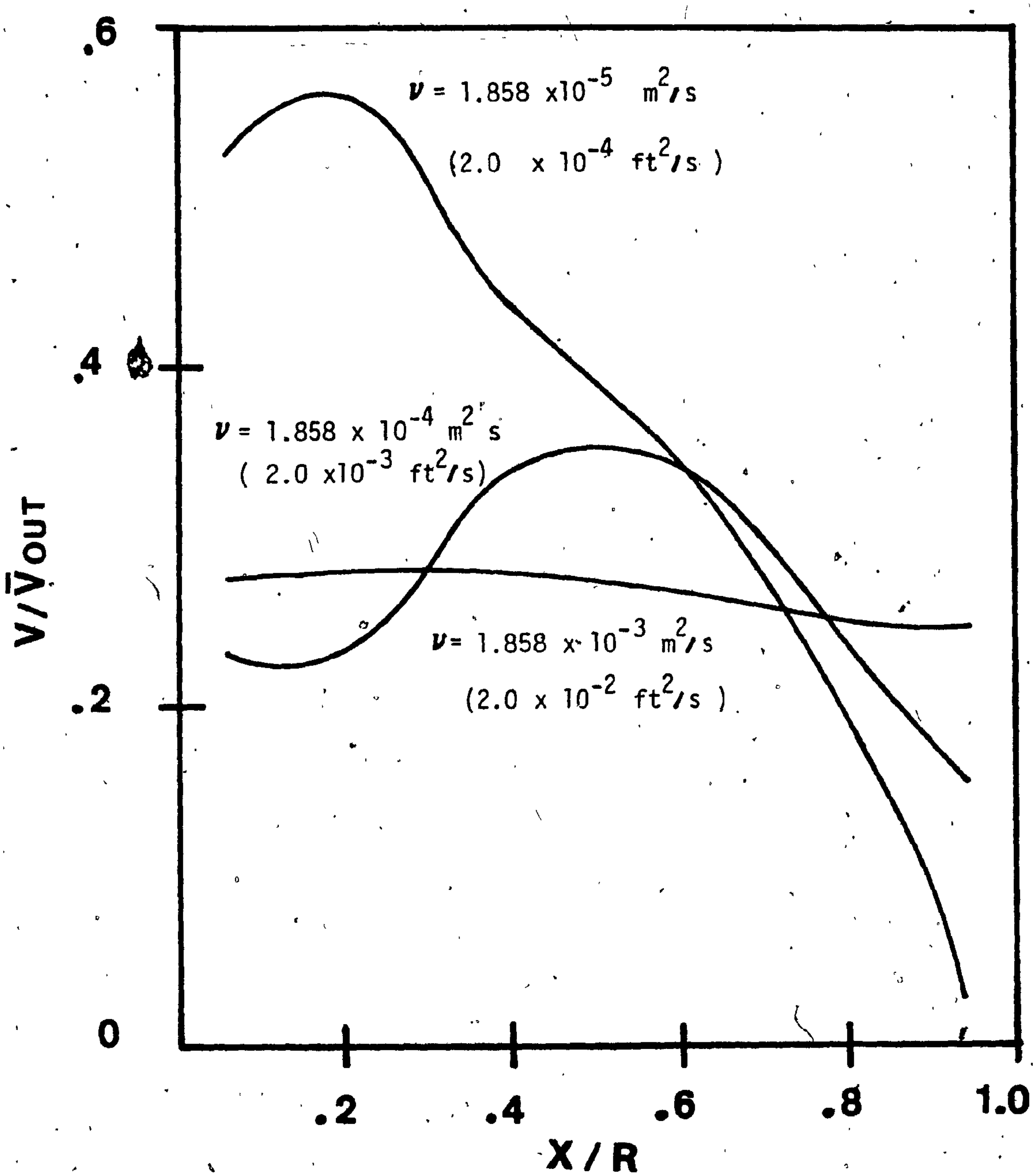

Figure 17: Axial Velocity Profiles at Radial Station Z_3 for Different Constant Viscosities.

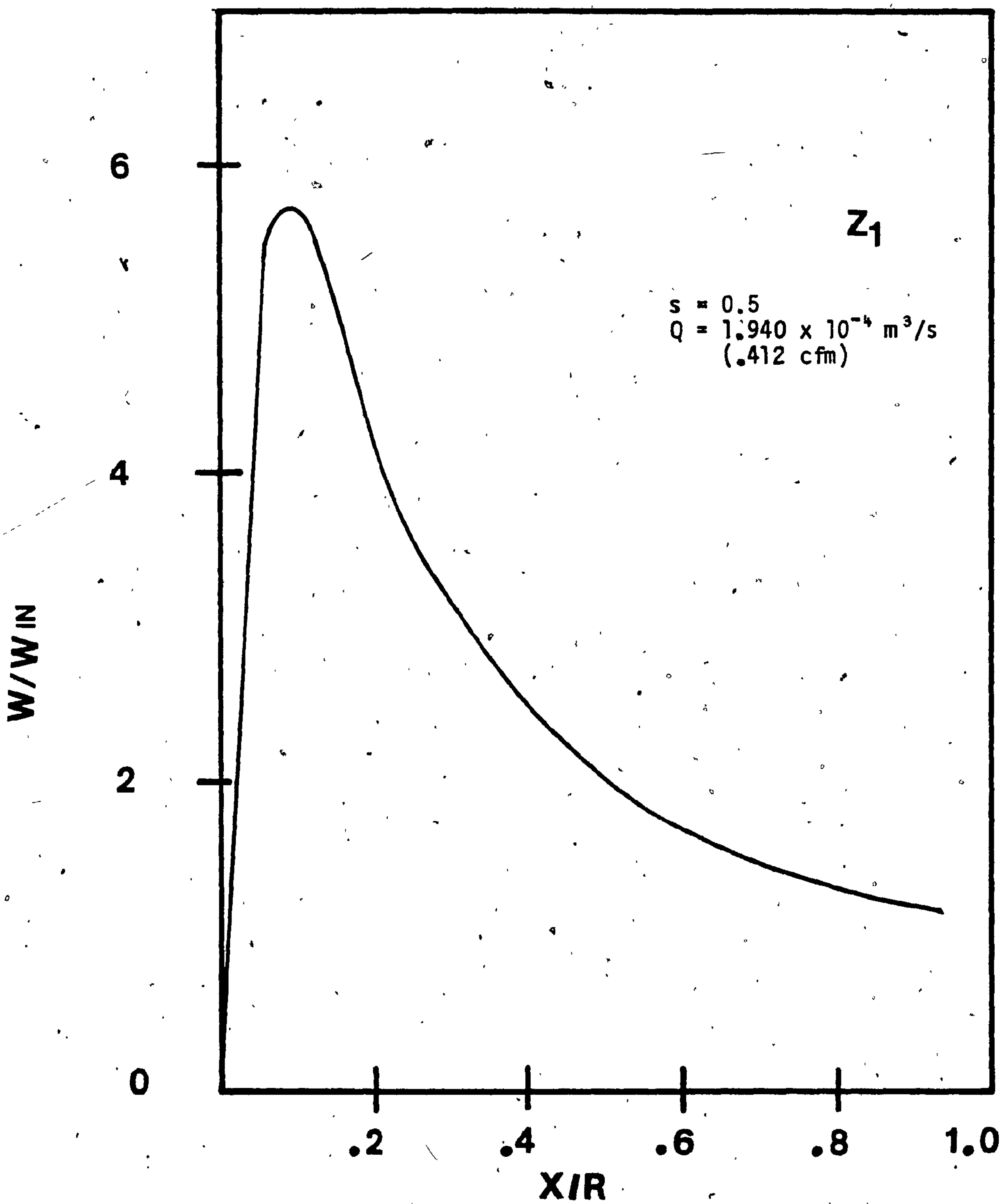

Figure 18: Tangential velocity Distribution for the Radial Station Z_1.

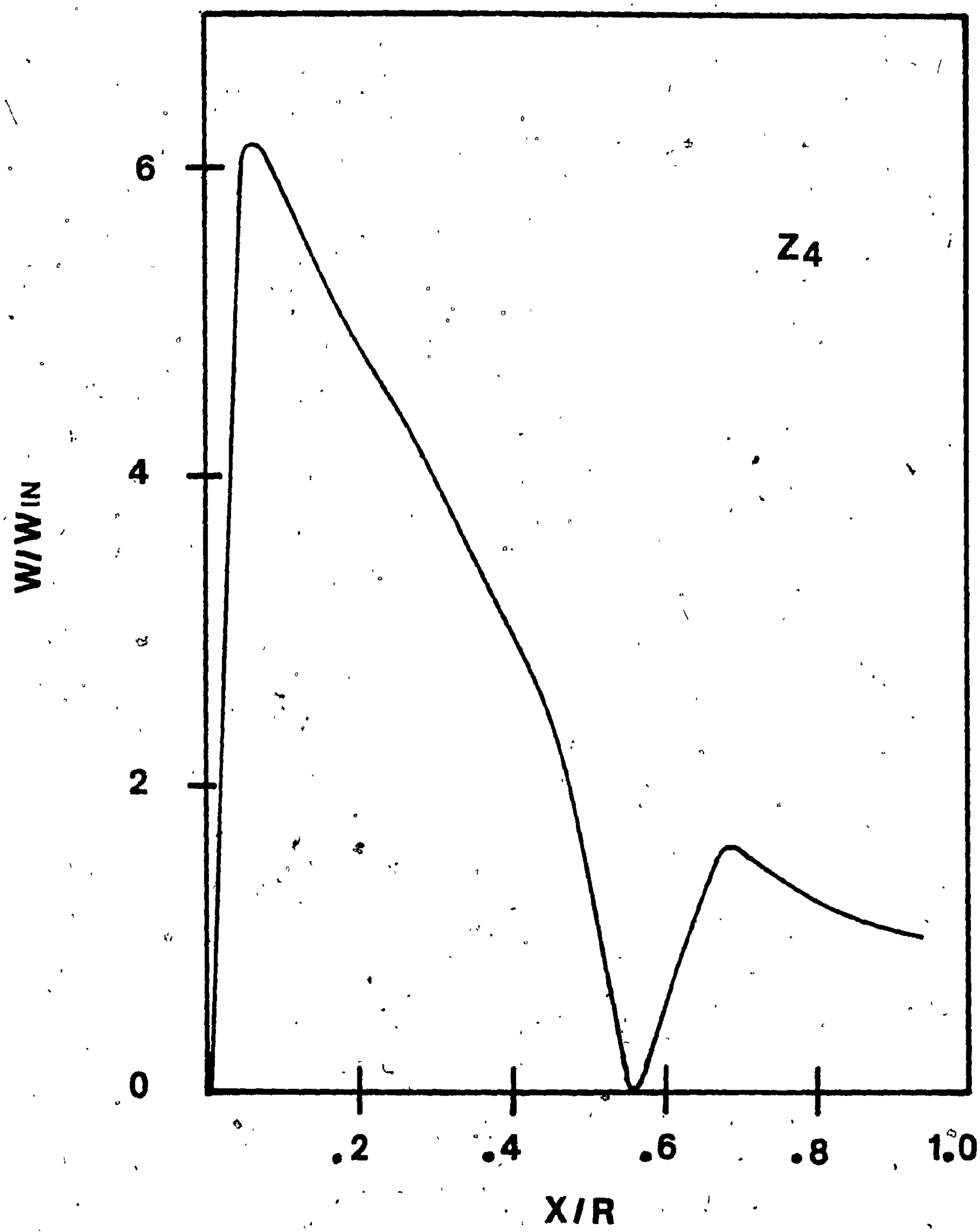

Figure 19: Tangential Velocity Distribution for Z_4.

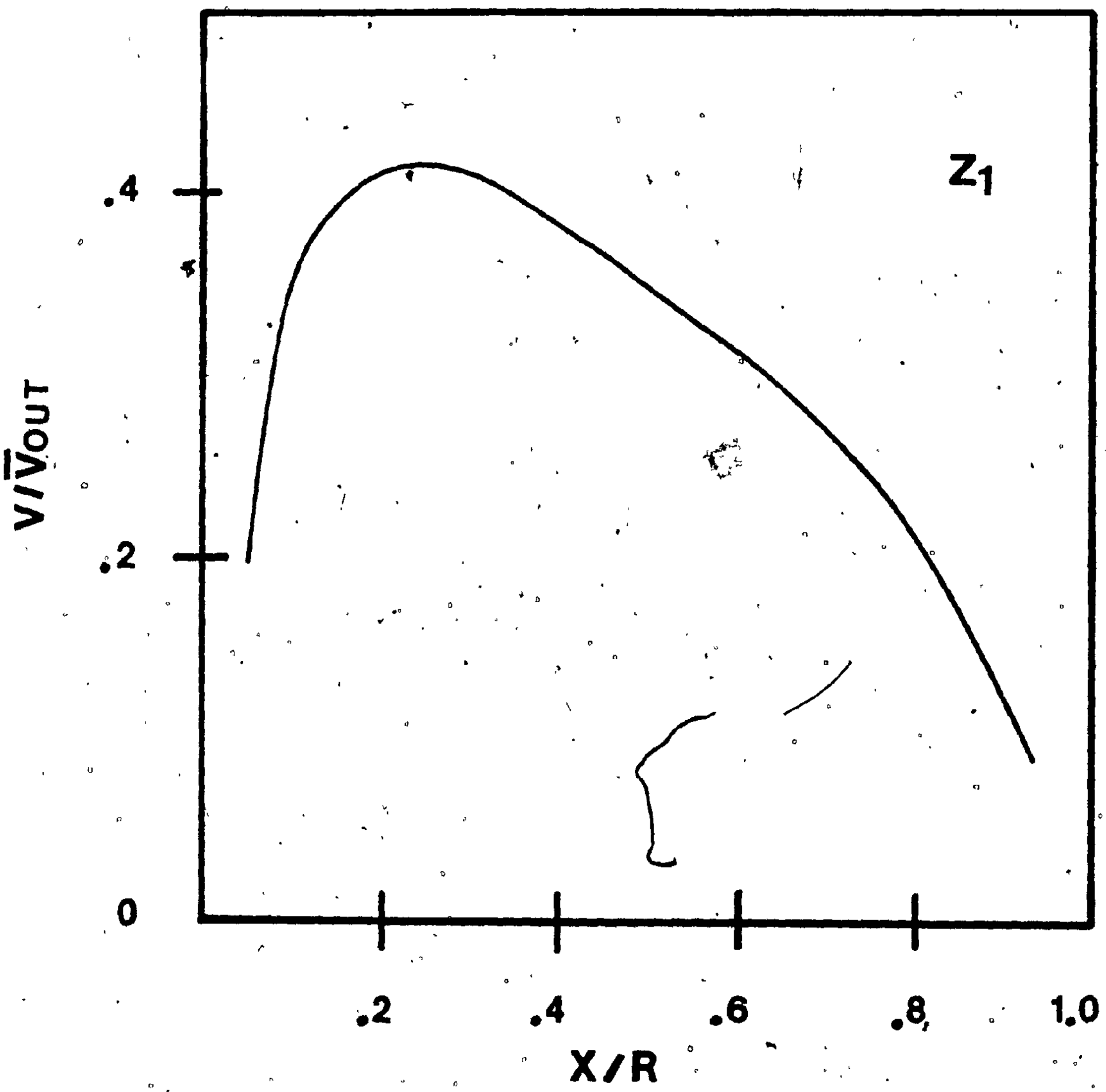

Figure 20: Axial Velocity profile for Z_1.

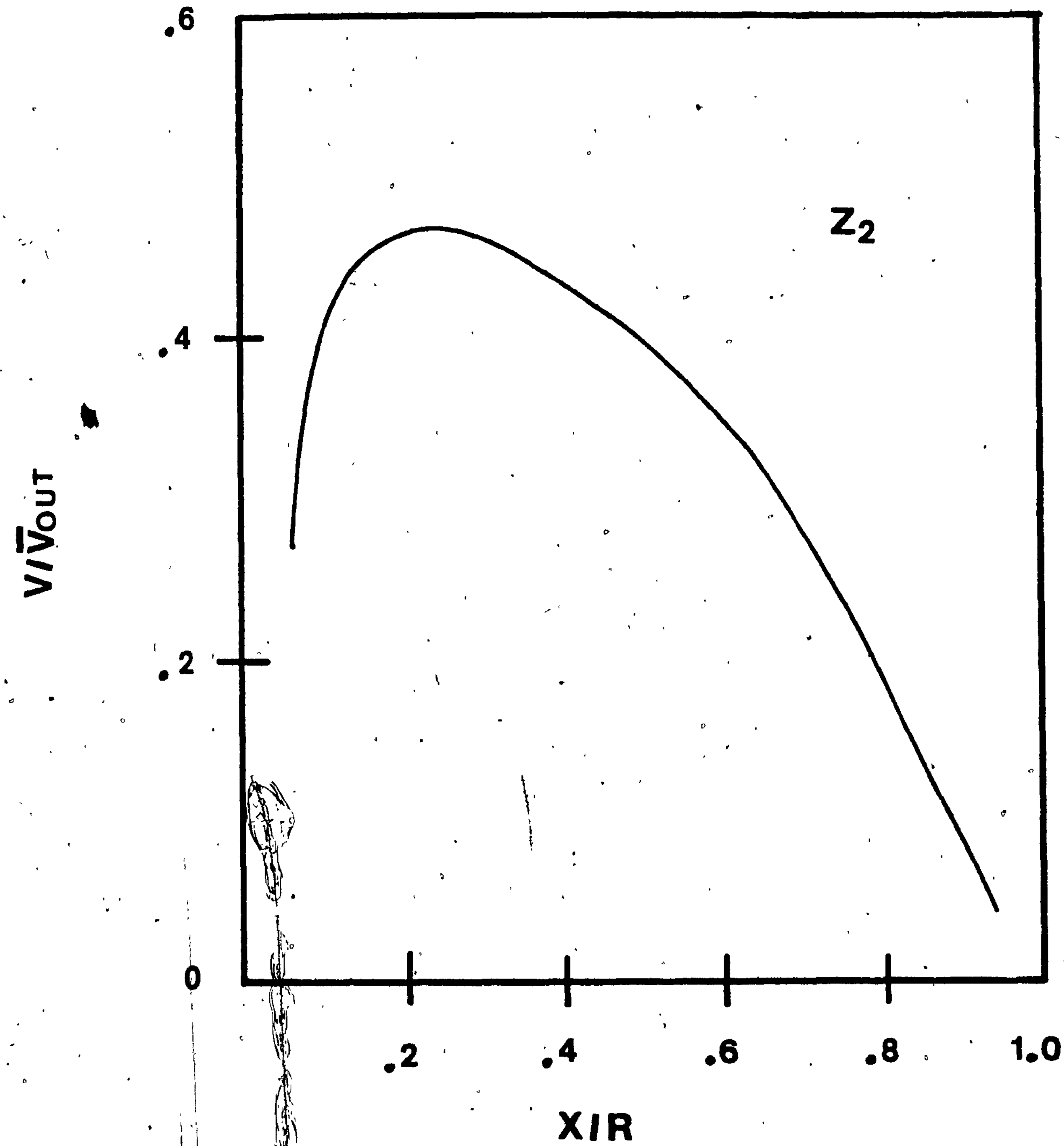

Figure 21: Axial velocity Distribution for Z_2.

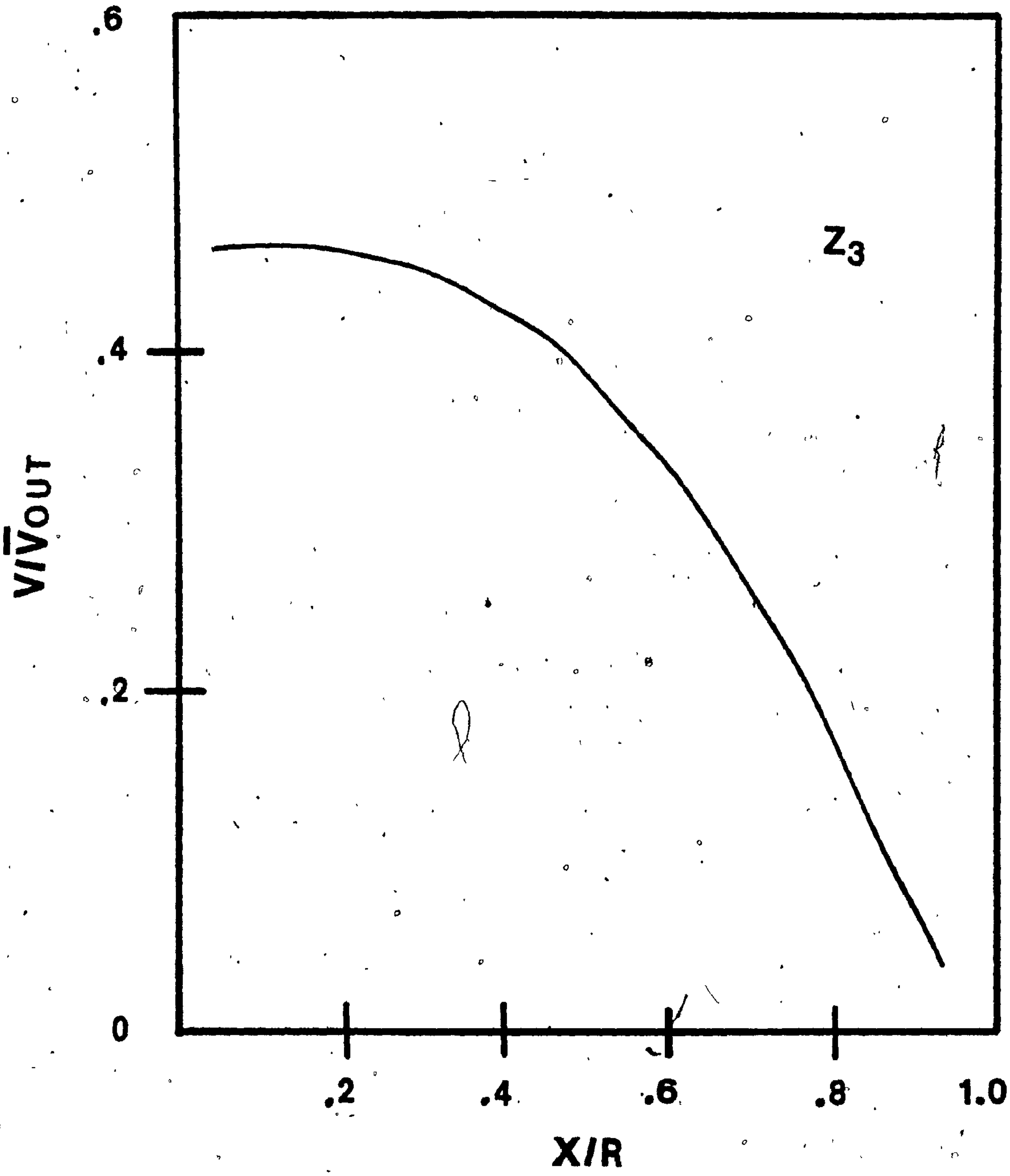

Figure 22: Axial Velocity Profile for Z_3.

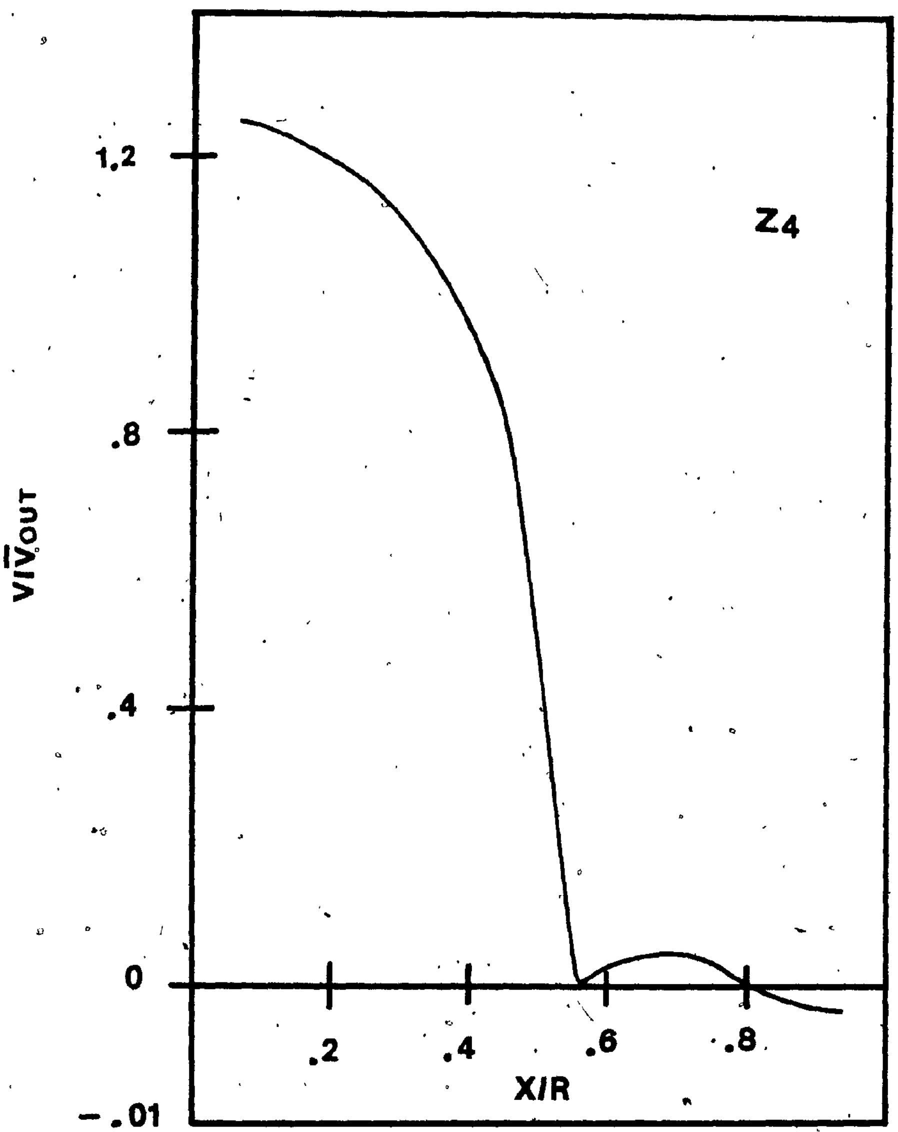

Figure 23: Axial velocity Profile for Z_4.

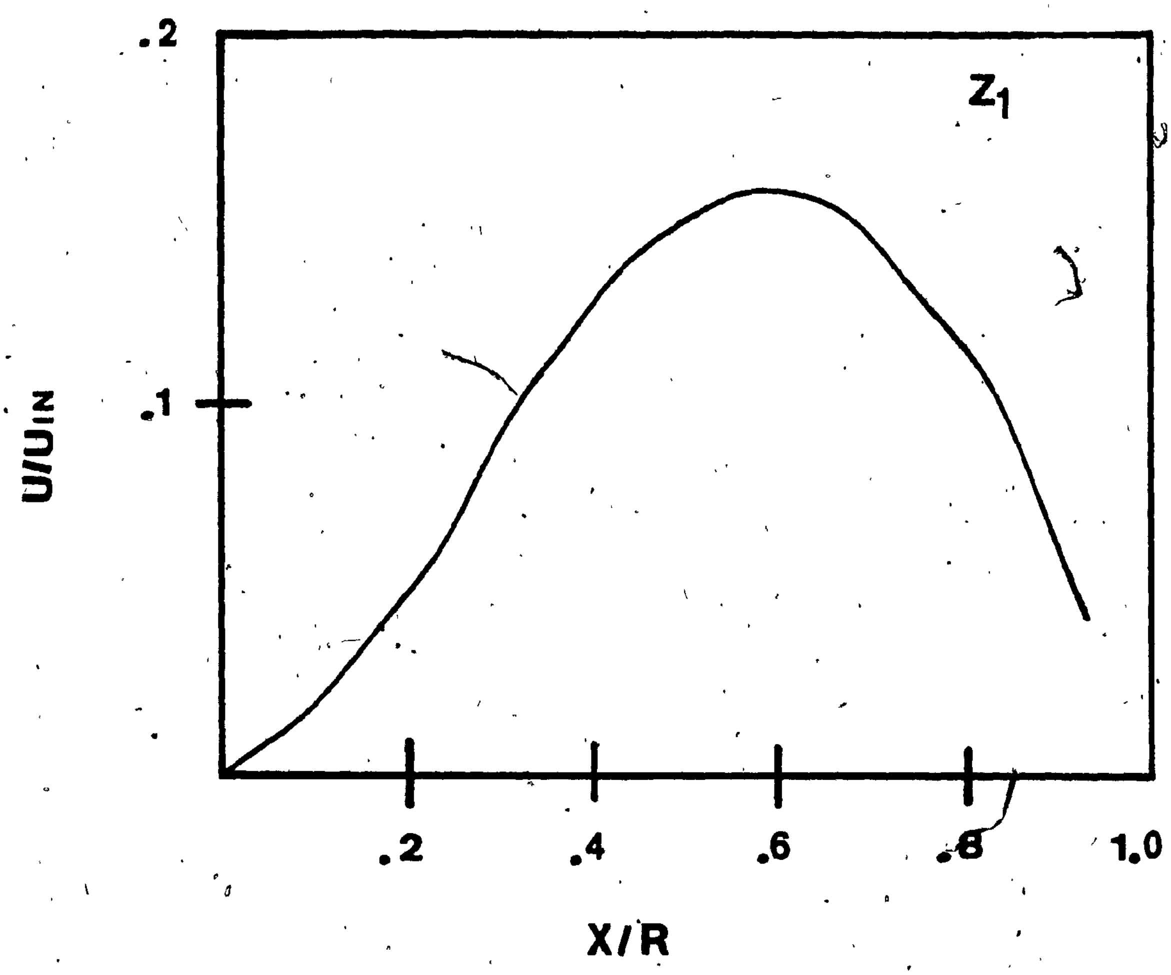

Figure 24: Radial Velocity Distribution for Z_1.

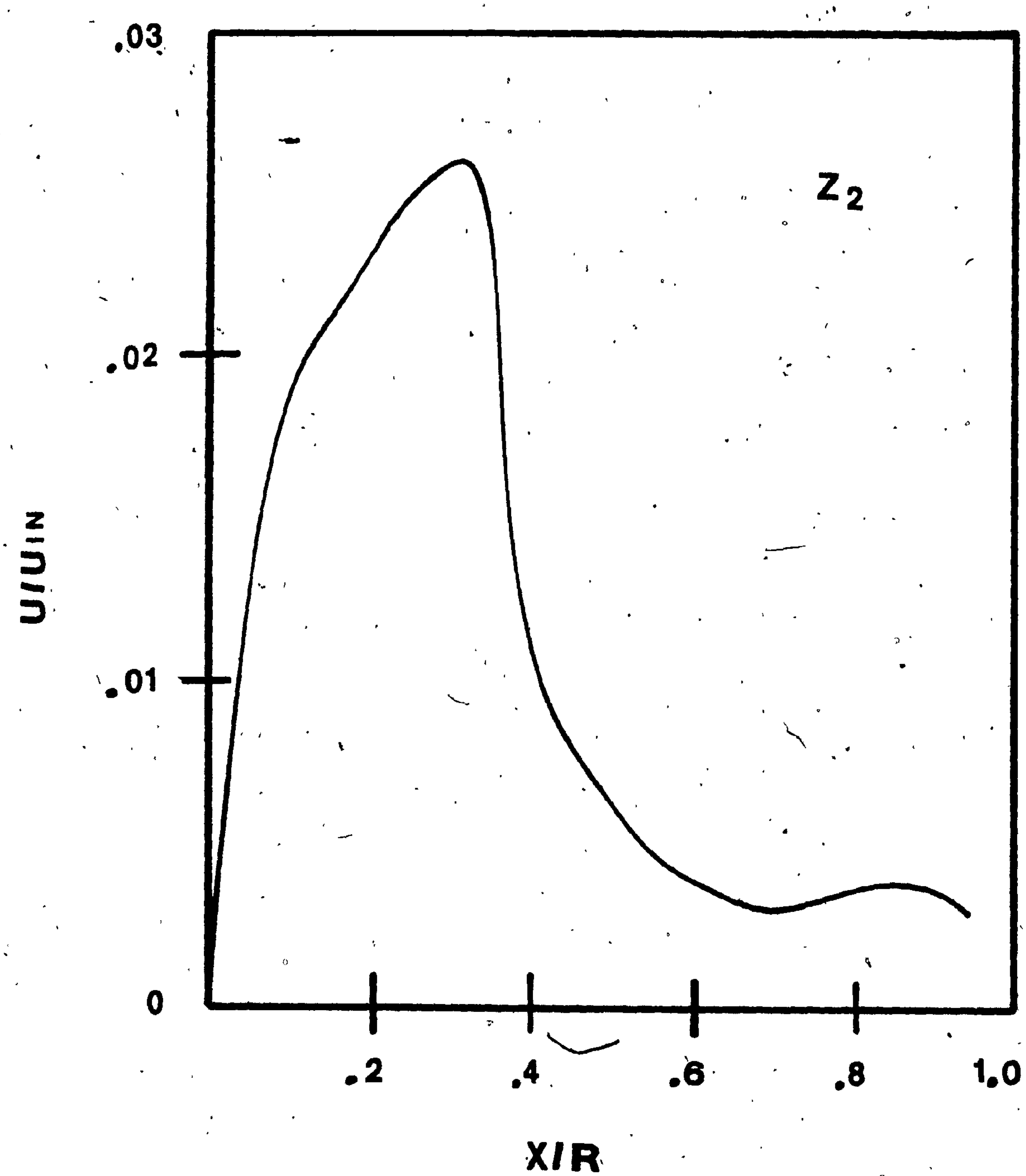

Figure 25: Radial Velocity Profile for Z_2.

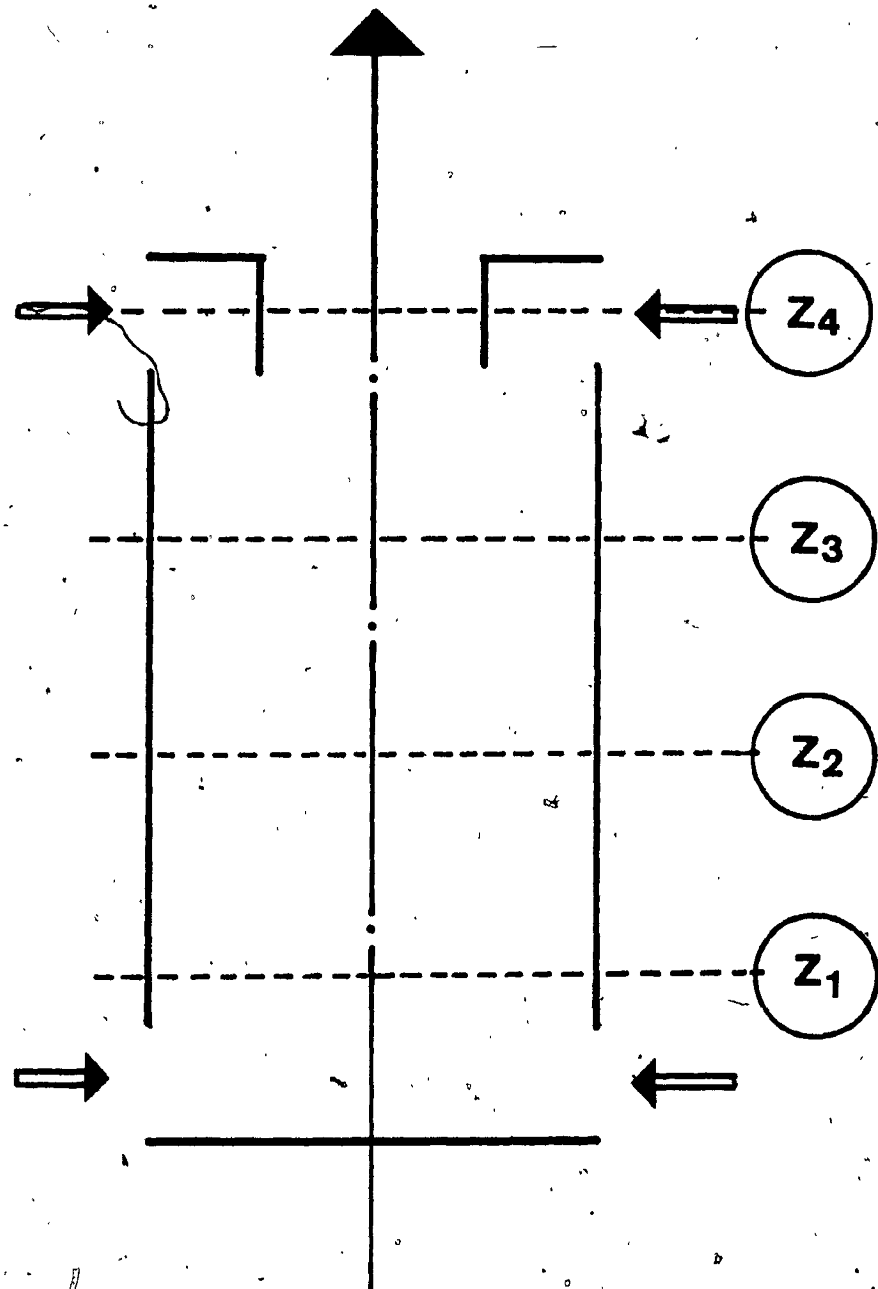

Figure 26: Schematic of two Sets of Inlets (Near the Top and Base Plates)
Cyclone Chamber and Arrangements of the Radial Stations.

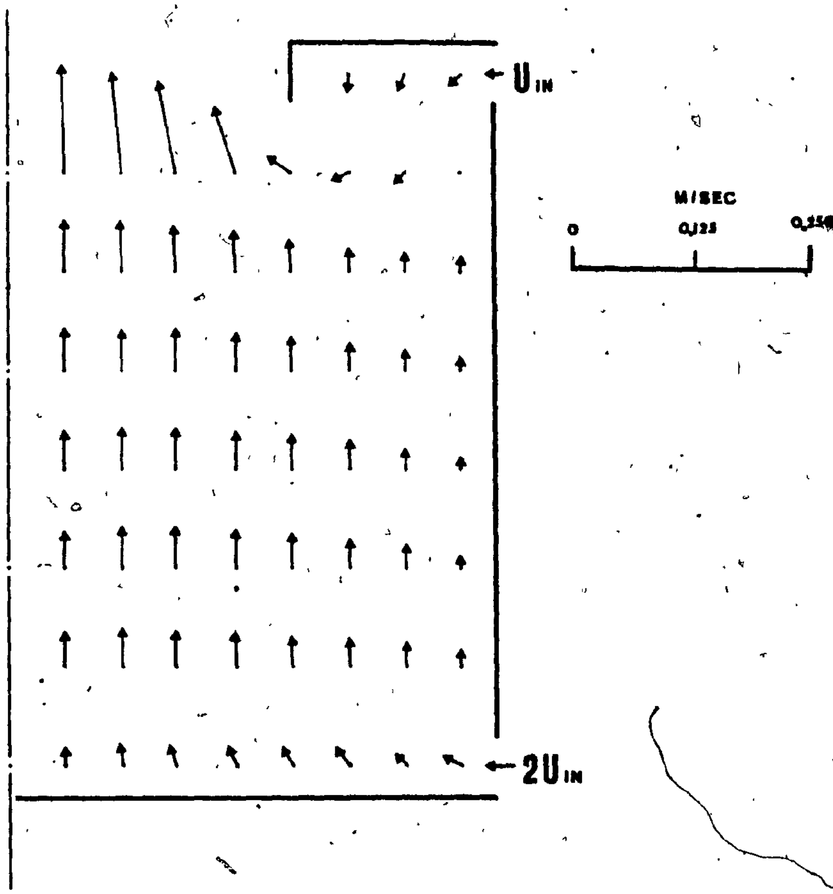

Figure 27: Computer Vector Graph for U and V Velocity Components with S = 0.5.

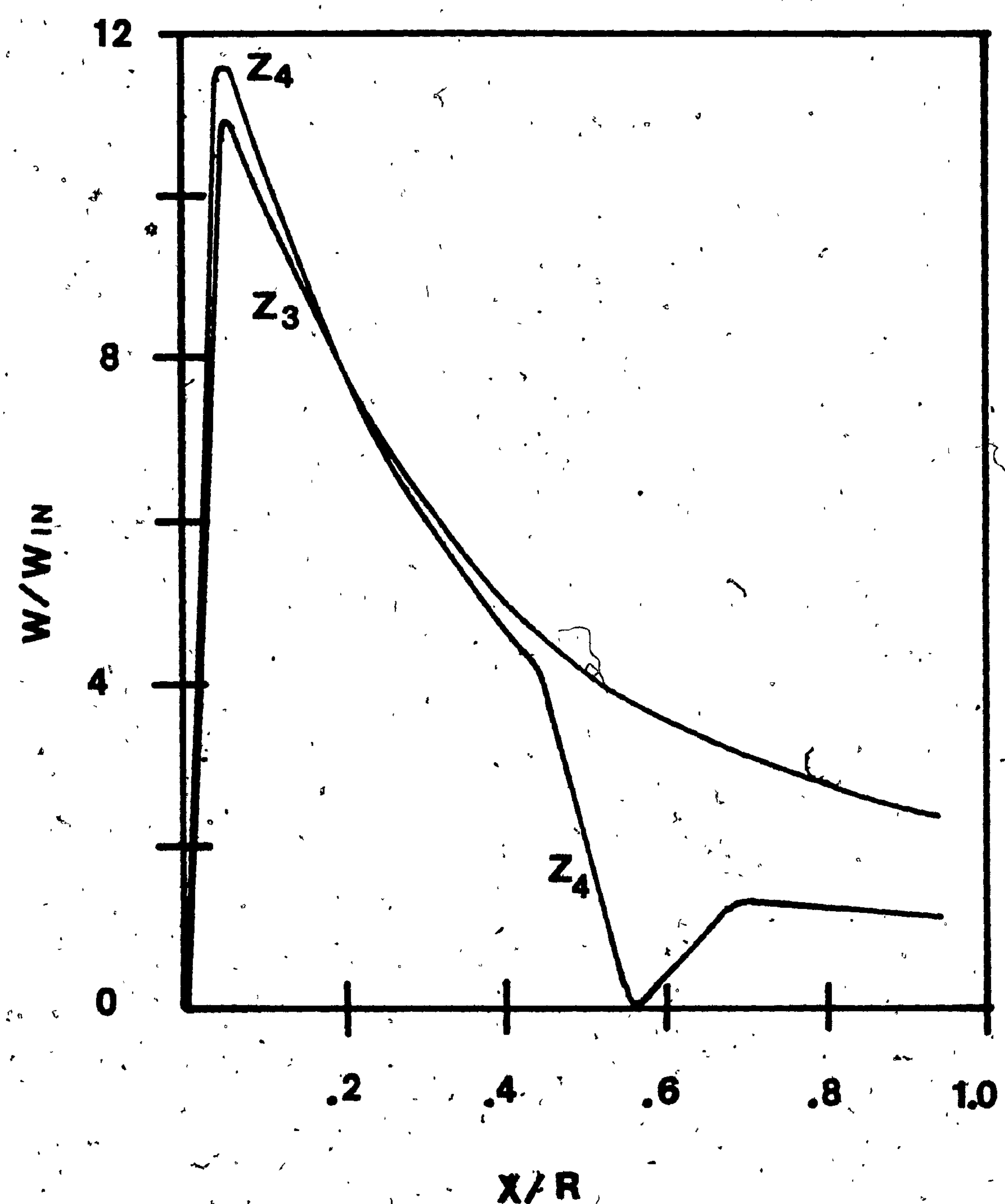

Figure 28: Tangential Velocity Profiles with S = 0.5 and Inlet Velocities of U_{IN} and 2 U_{IN} on Top and Bottom Respectively.

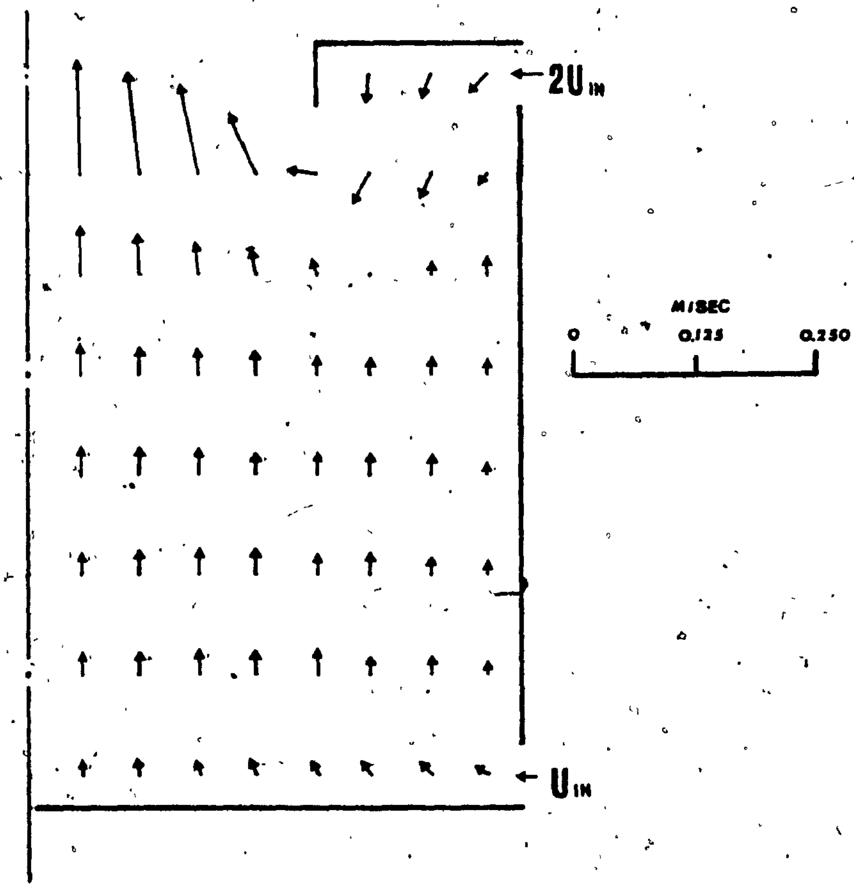

Figure 29: Computer Vector Graph for U and V Velocity Components with S = 0.5.

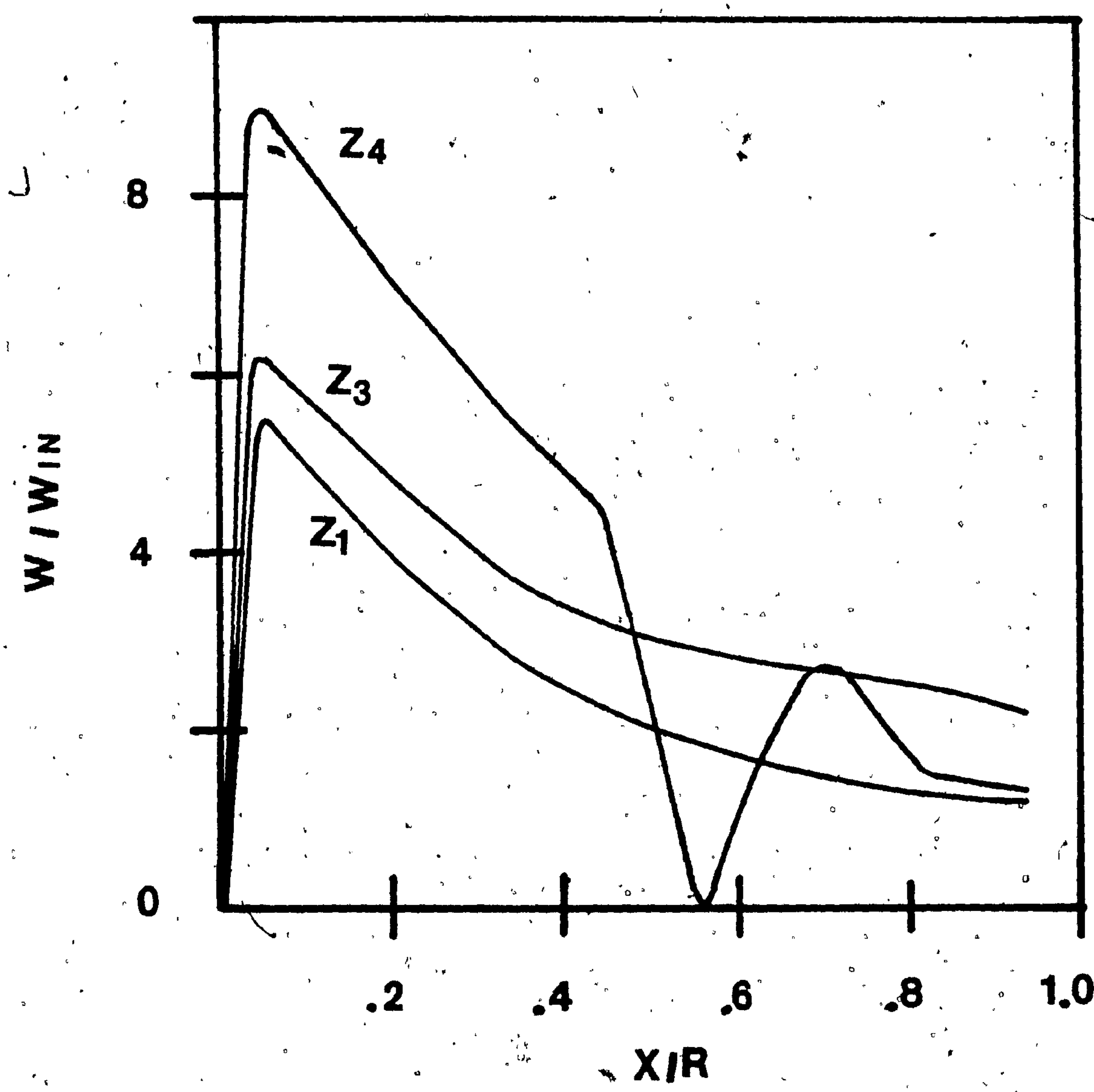

Figure 30: Tangential Velocity Profiles with s = 0.5 and Inlet Velocities of 2 U_{IN} and U_{IN} on the Top and Bottom Respectively.

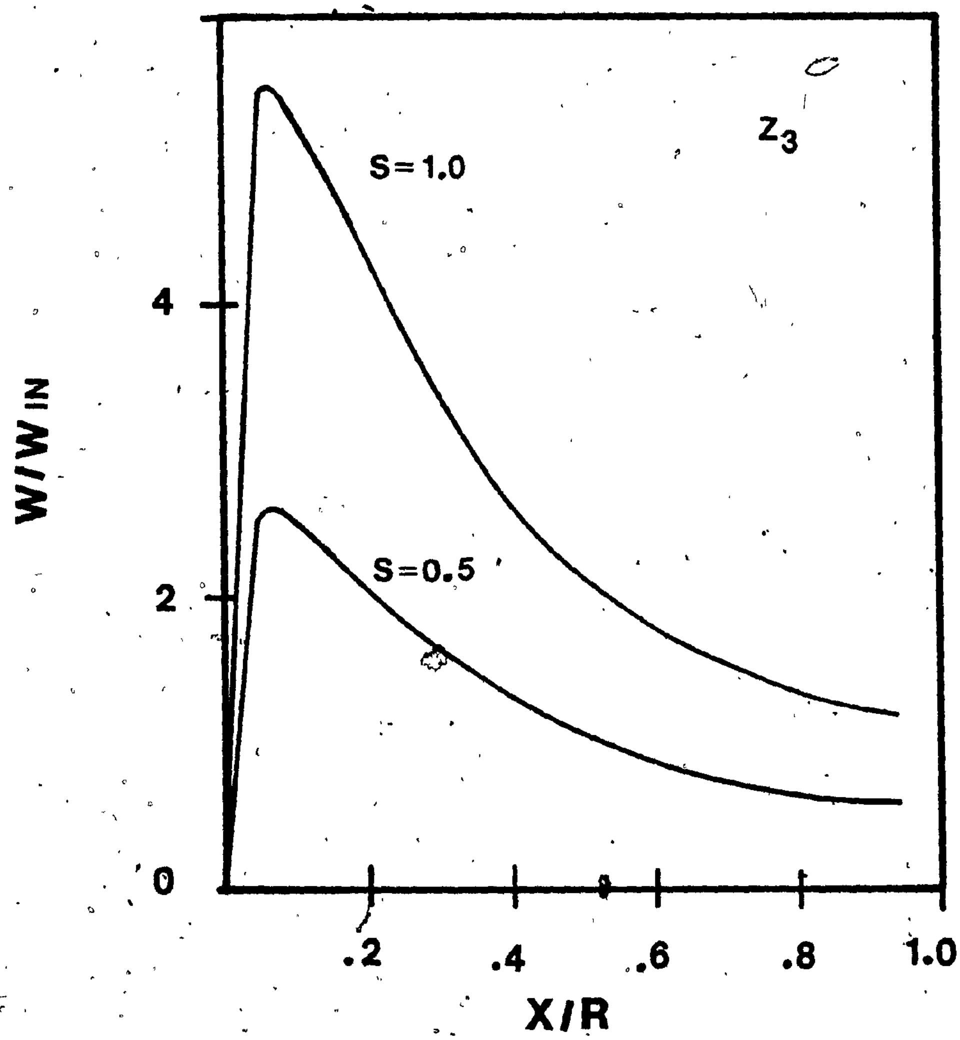

Figure 31: Tangential Velocity Distribution for the Radial Station Z_3 for the Inlet Swirl Strengths of 0.5 and 1.0.

APPENDIX A

The 4 terms on the right of each of the equations (3.1.1) are defined by:

<u>U - equation</u>

$$FUX = \frac{1}{4\Delta x}\Big[(U_{i,j}+U_{i+1,j})^2 + \alpha\,|U_{i,j}+U_{i+1,j}|\,(U_{i,j}-U_{i+1,j})$$

$$- (U_{i-1,j}+U_{i,j})^2 - \alpha|U_{i-1,j}+U_{i,j}|\,(U_{i-1,j}-U_{i,j})\Big]$$

$$FUY = \frac{1}{4\Delta y}\Big[(V_{i,j}+V_{i+1,j})\,(U_{i,j}+U_{i,j+1}) + \alpha|V_{i,j}+V_{i+1,j}|$$

$$(U_{i,j}-U_{i,j+1}) - (V_{i,j-1}+V_{i+1,j-1})\,(U_{i,j-1}+U_{i,j})$$

$$- \alpha|V_{i,j-1}+V_{i+1,j-1}|\,(U_{i,j-1}-U_{i,j})\Big]$$

$$FUC = \frac{1}{8\Delta x(i-1)}\Big[(U_{i,j}+U_{i+1,j})^2 + (U_{i-1,j}+U_{i,j})^2$$

$$+ \alpha|U_{i,j}+U_{i+1,j}|\,(U_{i,j}-U_{i+1,j})$$

$$+ \alpha|U_{i-1,j}+U_{i,j}|\,(U_{i-1,j}+U_{i,j})\Big] - \frac{1}{4\Delta x(i-1)}$$

$$(W_{i,j}+W_{i+1,j})^2$$

$$VISX = \nu\Big[\frac{1}{\Delta x^2}(U_{i+1,j}-2U_{i,j}+U_{i-1,j}) + \frac{1}{\Delta y^2}(U_{i,j+1}-2U_{i,j}+U_{i,j-1})$$

$$+ \frac{1}{2\Delta x^2(i-1)}(U_{i+1,j}-U_{i-1,j}) - \frac{U_{i,j}}{\Delta x^2(j-1)^2}\Big]$$

<u>V - equation</u>

$$FVX = \frac{1}{4\Delta x}\Big[(U_{i,j} + U_{i,j+1})(V_{i,j} + V_{i+1,j}) + \alpha|U_{i,j} + U_{i,j+1}|(V_{i,j} - V_{i+1,j}) - (U_{i-1,j} + U_{i-1,j+1})(V_{i-1,j} + V_{i,j}) - \alpha|U_{i-1,j} + U_{i-1,j+1}|(V_{i-1,j} - V_{i,j})\Big]$$

$$FVY = \frac{1}{4\Delta y}\Big[(V_{i,j} + V_{i,j+1})^2 + \alpha|V_{i,j} + V_{i,j+1}|(V_{i,j} - V_{i,j+1}) - (V_{i,j-1} + V_{i,j})^2 - \alpha|V_{i,j-1} + V_{i,j}|(V_{i,j-1} - V_{i,j})\Big]$$

$$FVC = \frac{1}{8\Delta x(i-1.5)}\Big[(U_{i,j} + U_{i,j+1})(V_{i,j} + V_{i+1,j}) + (U_{i-1,j} + U_{i-1,j+1})(V_{i-1,j} + V_{i,j}) + \alpha|U_{i,j} + U_{i,j+1}|(V_{i,j} - V_{i+1,j}) + \alpha|U_{i-1,j} + U_{i-1,j+1}|(V_{i-1,j} - V_{i,j})\Big]$$

$$VISY = \nu\Big[\frac{1}{\Delta x^2}(V_{i+1,j} - 2V_{i,j} + V_{i-1,j}) + \frac{1}{\Delta y^2}(V_{i,j+1} - 2V_{i,j} + V_{i,j-1}) + \frac{1}{2\Delta x^2(i-1.5)}(V_{i+1,j} - V_{i-1,j})\Big]$$

W - equation

$$FWX = \frac{1}{2\Delta x}\Big[U_{i,j}(W_{i,j} + W_{i+1,j}) + \alpha|U_{i,j}|\ (W_{i,j} - W_{i+1,j})$$

$$- U_{i-1,j}\ (W_{i-1,j} + W_{i,j}) - \alpha|U_{i-1,j}|\ (W_{i-1,j} - W_{i,j})\Big]$$

$$FWY = \frac{1}{2\Delta y}\Big[V_{i,j}\ (W_{i,j} + W_{i,j+1}) + \alpha|V_{i,j}|\ (W_{i,j} - W_{i,j+1})$$

$$- V_{i,j-1}\ (W_{i,j-1} + W_{i,j}) - \alpha|V_{i,j-1}|\ (W_{i,j-1} - W_{i,j})\Big]$$

$$FWC = \frac{1}{2\Delta x(i-1.5)}\Big[U_{i,j}(W_{i,j} + W_{i+1,j}) + U_{i-1,j}\ (W_{i-1,j} + W_{i,j})$$

$$+ \alpha|U_{i,j}|\ (W_{i,j} - W_{i+1,j}) + \alpha|U_{i-1,j}|\ (W_{i-1,j} - W_{i,j})\Big]$$

$$VISZ = \nu\Big[\frac{1}{\Delta x^2}\ (W_{i+1,j} - 2W_{i,j} + W_{i-1,j}) + \frac{1}{\Delta y^2}\ (W_{i,j+1} - 2W_{i,j} + W_{i,j-1})$$

$$+ \frac{1}{2\Delta x^2(i-1.5)}\ (W_{i+1,j} - W_{i-1,j}) - \frac{W_{i,j}}{\Delta x^2(i-1.5)^2}\Big]$$

Terms here are evaluated at time level t.

APPENDIX B

```
      PROGRAM CYCLONE(INPUT,OUTPUT,TAPE60,TAPE5,TAPE6=OUTPUT)
C     ==================================================================
C
C     PROGRAM CYCLONE COMPUTES THE ASSUMED 2-D AXISYMMETRIC SWIRLING
C     FLOW WITHIN A CYCLONE CHAMBER .
C     THE DATA TO BE ENTERED IS,
C        DELX       IS THE MESH SIZE IN THE X-D
C        DELY       IS THE MESH SIZE IN THE Y-D
C        IBAR       NUMBER OF DIVISIONS IN THE X-D
C        JBAR       NUMBER OF DIVISIONS IN THE Y-D
C        IOUT       NUMBER OF COMPUTATIONAL CELLS FOR THE EXIT PORT
C        ALPHA      CONVERGENCE AND STABILITY PARAMETER TAKING A VALUE
C                   BETWEEN(0,1).
C        DELT       TIME INCREMENT
C        MCYR       NUMBER OF FORWARD IN TIME FRAMES THAT SHOULD BE TAKEN
C                   FOR STEADY STATE CONDITIONS
C        LPR        SELECTION PRINT INTERMEDIATE FLOWFIELDS VALUES
C        UINITL     INLET RADIAL VELOCITY
C        WINITL     INLET TANGENTIAL VELOCITY
C
C     ==================================================================
      INTEGER CYCLE,THRU
      REAL NU
      DIMENSION U(15,15),V(15,15),W(15,15),P(15,15),UN(15,15),VN(15,15)
     +,WN(15,15)
C-----------------------------------------------------------------------
C     P A R A M E T E R  S E T T I N G
      DATA EPSI,GX,GY,CYL, OMG
     +/5.E-3,0.0,0.0,1.0,1.7/
      DZRO=1.0
C     G E O M E T R I C   P A R A M E T E R S
      DELX=0.026
      DELY=0.105
      JBAR=8
      IBAR=8
      JINT=2
      JINB=2
      IOUT=5
      PI=3.14159
C     F L U I D   D Y N A M I C   P A R A M E T E R S
      NU=2.E-4
C     C O N V E R G E N C E   A N D   A C C U R A C Y   P A R A M E T E R S
      ALPHA=1.0
      DELT=0.0014
      MCYR=2000
C     P R I N T I N G   I N S T R U C T I O N S
      LPR=300
      IWRITE=0
C     B O U N D A R Y   C O N D I T I O N   I N S T R U C I I O N S
C     I N L E T   V E L O C I T I E S
      UINITL=-2.08
      WINITL=1.04
      SWRAT=WINITL/UINITL
C-----------------------------------------------------------------------
```

```
      PRINT 9001,UINITL,WINITL,JINT,JINB,SWRAT
 9001 FORMAT(1X,* UINITL = *,E14.4,/,*WINITL = *,E14.4,/,*-JINT = *,I2
     +,/,* JINB = *,I2,/,* SWRAT = *,E14.4,//)
      LSTEP=LPR
      HEIGT=JBAR*DELY
C
      JINBM1=JINB-1
      RLARGE=(IBAR   )*DELX
      AREAIN=2*(IBAR)*DELX*(JINT-JINBM1)*DELY*PI
      AREAOUT=((IOUT-1)*DELX)**2  *PI
      AREACH=((IBAR   )*DELX)**2*PI
      AREARAT=AREAIN/AREAOUT
      VOUT=-UINITL*AREARAT
C     R E Y N O L D S   N U M B E R   B A S E D   O N   C H A M B E R S
C     D I A M E T E R   A N D   A V E R A G E   C H .   V E L O C I T Y.
      VCHAMB=VOUT*AREAOUT/AREACH
      REYNUM=VCHAMB*RLARGE/NU
      PRINT 91,RLARGE,NU,AREAIN,AREAOUT,AREACH,AREARAT,VOUT,VCHAMB,
     1    REYNUM
C-----------------------------------------------------------------------
      IMAX = IBAR+2
      JMAX = JBAR+2
      IM1 = IBAR+1
      JM1 = JBAR+1
      IM2=IBAR
      JM2 = JBAR

      JTHR=(JMAX-1)-(JINT-JINB)
      THRH=JMAX-JTHR
      JTHRM1=JTHR-1
      RDX=1./DELX
      RDY=1./DELY
      BETA=OMG/(2.*DELT*(RDX**2 + RDY**2))
C     I N I T I A L I S A T I O N
C-----------------------------------------------------------------------
      T = 0
       ITER=0
       CYCLE=0
C     G U E S S   I N I T I A L   V E L O C I T I E S
      DO 560 I=1,IMAX
      DO 560 J=1,JMAX
      U(I,J) = 0.
      V(I,J) = 0.
      W(I,J) = 0.
  560   CONTINUE
C-----------------------------------------------------------------------
C     -------------------------------------------------------------------

        ASSIGN  5000 TO KRET
      GO TO 2000
 1000 CONTINUE
       ITER=0
       FLG=1.0
        ASSIGN  3000 TO KRET
```

```
C     A P P L Y   M O M E N T A   E Q U A T I O N S   F O R   T I M E
C     A D V A N C E D   U , V , W
C------------------------------------------------------------------------
      CALL TIMESTP(DELX,DELY,DELT,P,CYL,ALPHA,GX,GY,NU,UN,VN,WN,
     +U,V,W,IM1,JM1,RDX,RDY)
C------------------------------------------------------------------------

 2000 CONTINUE

C     ---------------------------------------------------------------------
C
C------------------------------------------------------------------------
C     G E N E R A L   B O U N D A R Y   C O N D I T I O N S
C
       DO 2200  J=1,JMAX
C
C     B O U N D A R Y   C O N D I T I O N S   O N   L E F T
      U(1,J)=0.0
      V(1,J)=V(2,J)
      W(1,J)=-W(2,J)
C
C     B O U N D A R Y   C O N D I T I O N S   O N   R I G H T
C
      IF(J.LE.JINT.AND.J.GE.JINB) GO TO 2200
       U(IM1,J)=0.0
       V(IMAX,J)= V(IM1,J)
      W(IMAX,J)=W(IM1,J)
2200    CONTINUE
C
C
       DO 2500 I=1,IMAX
C
C     B O U N D A R Y   C O N D I T I O N S   O N   T O P
C
      IF(I.LE.IOUT) GO TO 2400
        V(I,JM1)=0.0
        U(I,JMAX)=U(I,JM1)
      W(I,JMAX)=W(I,JM1)
 2400 CONTINUE
C     B O U N D A R Y   C O N D I T I O N S   O N   B O T T O M
C
      V(I,1)=0.
        U(I,1)=U(I,2)
      W(I,1)=W(I,2)
2500    CONTINUE

C
C     S P E C I A L   B O U N D A R Y   C O N D I T I O N S
C------------------------------------------------------------------------
C


C     E X I T   T H R O A T   W A L L
      V(IOUT+1,JTHRM1)=0.
      DO 2810 J=JTHR,JMAX
      U(IOUT+1,J)=0.
      W(IOUT+1,J)=0.
      V(IOUT+1,J)=0.
```

```
      U(IOUT,J)=0.
 2810 CONTINUE


C     O U T L E T  B O U N D A R Y   C O N D I T I O N S
C     C O M P U T A T I O N  O F  T H E  I N  A N D  O U T  F L U X E S
      FLUXIN=0.
      DO 2811 J=JINB,JINT
      V(IMAX,J)=0.
      U(IMAX,J)= UINITL
      U(IM1,J)= UINITL
      W(IMAX,J)=WINITL
      FLUXIN=FLUXIN-2.*PI*IBAR*DELY*DELX*U(IM1,J)
 2811 CONTINUE
      FLUXOUT=3.14159*DELX**2*V(2,JM2)
      DO 6113 I=3,IOUT
 6113  FLUXOUT=FLUXOUT+2.*3.14159*(FLOAT(I)-1.5)*DELX**2*V(I,JM2)
      IF(ITER.GT.0)GO TO 2813
      VINC=(FLUXIN-FLUXOUT)/AREAOUT
      DO 2817 I=2,IOUT
      V(I,JM1)=V(I,JM2)+VINC
      V(I,JMAX)=V(I,JM1)
      U(I,JMAX)=U(I,JM1)
 2817 W(I,JMAX)=W(I,JM1)
 2813 CONTINUE
C-----------------------------------------------------------------------
C     P R E S S U R E  I T E R A T I O N  A N D  P , U , V
C-----------------------------------------------------------------------
       GO TO KRET (3000,5000)
3000     CONTINUE
       IF (FLG.EQ.0) GOTO4000
       ITER=ITER+1
      STORIT=ITER
       IF(ITER.LT.900)GOTO  3050
       IF(CYCLE.LT.20)GOTO 4000
C     T E R M I N A T I O N  C O N D I T I O N
       T=1E+10
       GOTO5000
3050    FLG=0.0
C     C H E C K  I F  C O N V E R G E N C E  H A S  B E E N
C     R E A C H E D
      SUMD=0.0
      DO 3500 J=2,JM1
      DO 3500 I=2,IM1
      D=RDX*(U(I,J)-U(I-1,J))+RDY*(V(I,J)-V(I,J-1))+CYL*(U(I,J)
     1 + U(I-1,J))/(2.*DELX*(FLOAT(I)-1.5))
      IF(ABS(D/DZRO).GE.EPSI)FLG=1.0
      DELP = -BETA*D
      P(I,J)=P(I,J)+DELP
      U(I,J)=U(I,J)+DELT*RDX*DELP
      U(I-1,J) = U(I-1,J) - DELT*RDX*DELP
      V(I,J)=V(I,J)+DELT*RDY*DELP
      V(I,J-1) = V(I,J-1)-DELT*RDY*DELP
      SUMD=SUMD+ABS(D)
 3500 CONTINUE
C
C     C H E C K P R I N T S  D U R I N G  P R E S S U R E  C Y C L E
```

```
      IWRITE=0
      IF(ITER.LE.2)IWRITE=1
      IF(CYCLE.GT.30.AND.CYCLE.LT.MCYR) IWRITE=0
      IF(IWRITE.EQ.1)GO TO 5152
C     R E T U R N   F R O M   P R I N T I N G   S E C T I O N
 3501 CONTINUE
      IWRITE=0
C
      GO TO 2000
4000   CONTINUE.
 5000 CONTINUE
C-----------------------------------------------------------------------
C     I N T E R M E D I A T E   P R I N T I N G
      IF(CYCLE.GE. MCYR-5) GO TO 5152
      KATA=CYCLE/LSTEP
      IF(KATA.EQ.1) LSTEP=LSTEP+LPR
      IF(KATA.EQ.1) GO TO 5152
               IF(CYCLE.GT.2 ) GO TO 5251
5152    CONTINUE
      CALL PRNT(ITER,T,CYCLE,U,V,W,P,SWRL,JMAX,IMAX)
      SUMU=0.0
      SUMV=0.0
      SUMW=0.0
      DO 6100 I=2,IM1
      DO 6100 J=2,JM1
      SUMU=SUMU+ABS(UN(I,J)-U(I,J))
      SUMV=SUMV+ABS(VN(I,J)-V(I,J))
      SUMW=SUMW+ABS(WN(I,J)-W(I,J))
6100     CONTINUE
      PRINT 90
      PRINT 91,U(3,4),V(3,4) ,W(3,4) ,STORIT,SUMU,SUMV,SUMW,SUMD
5251     CONTINUE

C     R E T U R N   T O   P R E S S U R E   I T E R A T I O N
C     C Y C L E   I F   T H E S E   W E R E   O N L Y
C     C H E C K P R I N T S
      IF(IWRITE.EQ.1)GO TO 3501
C-----------------------------------------------------------------------
C------------REPACKAGING
       DO 6101 I=1,IMAX
       DO 6101 J=1,JMAX
       UN(I,J)=U(I,J)
       VN(I,J)=V(I,J)
      WN(I,J)=W(I,J)
 6101 CONTINUE
C     C O M P U T A T I O N   O F   I N   A N D   O U T   F L U X E S
      FLUXIN=0.0
      DO 6110 J=JINB,JINT
 6110 FLUXIN=FLUXIN-2.*PI*IBAR*DELY*DELX*U(IM1,J)
      FLUXOUT=3.14159*DELX**2*V(2,JM1)
      DO 6111 I=3,IOUT
 6111  FLUXOUT=FLUXOUT+2.*3.14159*(I-1.5)*DELX**2*V(I,JM1)
      FLUXRAT=FLUXIN/FLUXOUT
      PRINT 91,U(3,4),V(3,4) ,W(3,4) ,STORIT,SUMU,SUMV,SUMW,SUMD
C-----------------------------------------------------------------------
C     A D V A N C E   T I M E   A N D   C Y C L E
C-----------------------------------------------------------------------
       T=T+DELT
      IF(T.GT.MCYR*DELT) GO TO 6500
       CYCLE=CYCLE+1
```

```
      GOTO 1000
 6500 CONTINUE
 9000 CONTINUE
C-----------------------------------------------------------------------
C       V E L O C I T Y  C R A P H E S
      CALL PLOT (U,V,IMAX,JMAX)
C-----------------------------------------------------------------------
      STOP
   90 FORMAT(///4X,*UMON   *,8X,*VMON    *,7X,*WMON    *,7X,*PRESS ITER*,
     14X,*SUMU*,10X,*SUMV*,10X,*SUMW*,10X,*SUMD*//)
   91 FORMAT(8E14.4)
  100  FORMAT(1X,8E11.4)
       END


       SUBROUTINE TIMESTP(DELX,DELY,DELT,P,CYL,ALPHA,GX,GY,NU,UN,VN,WN,
      +U,V,W,IM1,JM1,RDX,RDY)

C      ==============================================================
C      T H I S  S U B R O U T I N E  C O M P U T E S  T H E  V A L U E S
C      O F  T H E  V E L O C I T Y  C O M P O N E N T S  F O R
C      J I M E  F R A M E  T + D T
C      ==============================================================
       REAL NU
       DIMENSION U(15,15),V(15,15),W(15,15),P(15,15),UN(15,15),VN(15,15)
      +,WN(15,15)

       DO 1100 I = 2,IM1
       DO 1100 J = 2,JM1
       FUX=((UN(I,J)+UN(I+1,J))*(UN(I,J)+UN(I+1,J))+ALPHA*ABS(UN(I,J)+UN(
      1I+1,J))*(UN(I,J)-UN(I+1,J))-(UN(I-1,J)+UN(I,J))*(UN(I-1,J)+UN(I,J)
      2)-ALPHA*ABS(UN(I-1,J) + UN(I,J)) *(UN(I-1,J)-UN(I,J)))/(4*DELX)
       FUY=((VN(I,J)+VN(I+1,J))*(UN(I,J) + UN(I,J+1))
      1 + ALPHA *      ABS(VN(I,J)+VN(I+1,J)) * (UN(I,J)-UN(I,J+1))
      2-(VN(I,J-1)+VN(I+1,J-1)) * (UN(I,J-1) + UN(I,J))
      3-ALPHA*ABS(VN(I,J-1)+VN(I+1,J-1))*(UN(I,J-1) - UN(I,J)))/(4.*DELY)
       FUC=CYL*((UN(I,J)+UN(I+1,J))*(UN(I,J)+UN(I+1,J))+(UN(I-1,J)+UN(I,J
      1))*(UN(I-1,J)+UN(I,J))
      2+ALPHA * ABS(UN(I,J) + UN(I+1,J)) * (UN(I,J)-UN(I+1,J))
      3+ALPHA * ABS(UN(I-1,J)+UN(I,J)) * (UN(I-1,J)-UN(I,J)))
      4 /(8.*DELX*FLOAT(I-1))
       FVX=((UN(I,J)+UN
      C                  (I,J+1))*(VN(I,J)+VN(I+1,J))+ALPHA*ABS(UN(I,J)+UN(
      1I,J+1))*(VN(I,J)-VN(I+1,J))-(UN(I-1,J)+UN(I-1,J+1))*(VN(I-1,J)+VN(
      2I,J))-ALPHA*ABS(UN(I-1,J)+UN(I-1,J+1))*(VN(I-1,J)-VN(I,J)))/(4.*DE
      3LX)
       FVY=((VN(I,J)+VN(I,J+1))*(VN(I,J)+VN(I,J+1))+ALPHA*ABS(VN(I,J)+VN
      1(I,J+1))*(VN(I,J)-VN(I,J+1))-(VN(I,J-1)+VN(I,J))*(VN(I,J-1)+VN(I,J
      2))-ALPHA*ABS(VN(I,J-1)+VN(I,J))*(VN(I,J-1)-VN(I,J)))/(4.*DELY)
       FVC=CYL*((UN(I,J)+UN(I,J+1))*(VN(I,J)+VN(I+1,J))+(UN(I-1,J)+UN(I-1,
      1,J+1))*(VN(I-1,J)+VN(I,J))+ALPHA*ABS(UN(I,J)+UN(I,J+1))*(VN(I,J)-V
      2N(I+1,J))+ALPHA*ABS(UN(I-1,J)+UN(I-1,J+1))*(VN(I-1,J)-VN(I,J)))
      3/(8.*DELX*(FLOAT(I-1)-.5))
       VISX= NU * ((UN(I+1,J)-2.*UN(I,J) + UN(I-1,J))/DELX**2+
      1          (UN(I,J+1)-2.*UN(I,J) + UN(I,J-1))/DELY**2
```

```
2 FCYL * ((UN(I+1,J)-UN(I-1,J))/(2.*DELX*DELX*FLOAT(I-1))
3  -UN(I,J)/(DELX*FLOAT(I-1))**2))
 VISY= NU* ((VN(I+1,J)-2.*VN(I,J) + VN(I-1,J)) DELX**2+
1              (VN(I,J+1)-2.*VN(I,J) + VN(I,J-1))/DELY**2
2 FCYL *   (VN(I+1,J)-VN(I-1,J))/(2.*DELX*DELX*(FLOAT(I)-1.5))) .
 FWX=(UN(I,J)*(WN(I,J)+WN(I+1,J))+ALPHA*(ABS(UN(I,J)))*(WN(I,J)-WN(
,       I+1,J))-UN(I-1,J)*(WN(I-1,J)+WN(I,J))-ALPHA*(ABS(UN(I-1,J)))*
,       (WN(I-1,J)-WN(I,J)))/(2*DELX)
 FWY=(VN(I,J)*(WN(I,J)+WN(I,J+1))+ALPHA*(ABS(VN(I,J)))*(WN(I,J)-WN(
,       I,J+1))-VN(I,J-1)*(WN(I,J-1)+WN(I,J)) ALPHA*(ABS(VN(I,J-1)))*
,       (WN(I,J-1)-WN(I,J)))/(2*DELY)
 FWC=(UN(I,J)*(WN(I,J)+WN(I+1,J))+UN(I-1,J)*(WN(I-1,J)+WN(I,J))+
,       ALPHA*(ABS(UN(I,J)))*(WN(I,J)-WN(I+1,J))+ALPHA*(ABS(UN(I-1,J)
,       ))*(WN(I-1,J)-WN(I,J)))/(2*DELX*(FLOAT(I)-1.5))
 VISZ=((WN(I+1,J)-2*WN(I,J)+WN(I-1,J))/(DELX**2)+(WN(I,J+1)-2*WN(I,
,        J)+WN(I,J-1))/(DELY**2)+(WN(I+1,J) -WN(I-1,J))/(2*(DELX**2)*(
, FLOAT(I)-1.5))-WN(I,J)/((DELX**2)*(FLOAT(I)-1.5)**2))*NU
 FACCU=(WN(I,J)+WN(I+1,J))**2/(4.*DELX*(FLOAT(I)-1))
 U(I,J)=UN(I,J)+DELT*((P(I,J)-P(I+1,J))*RDX+GX-FUX-FUY-FUC+VISX+
,           FACCU)
 V(I,J)= VN(I,J)+DELT*((P(I,J)-P(I,J+1))*RDY + GY-FVX-FVY-FVC+VISY)
 W(I,J)=WN(I,J)+DELT*(-FWX-FWY-FWC+VISZ)
1100 CONTINUE
 RETURN
 END
 SUBROUTINE PRNT(ITER,T,CYCLE,U,V,W,P,SWRL,IMAX,JMAX)
C    ================================================================
C    S U B R O U T I N E   P R N T   P R I N T S  T H E   U , V , W A N D
C    P   F I E L D   V A L U E S
C    ================================================================
 DIMENSION U(15,15),V(15,15),W(15,15),P(15,15)
 INTEGER CYCLE
 PRINT 53,ITER,T ,CYCLE
  WRITE(6,48)
 DO 7001 J=1,JMAX
 JMMJ=JMAX-J+1
  WRITE(6,47)  (U(I,JMMJ),I=1,IMAX)
7001  CONTINUE
  WRITE(6,49)
  DO 7002 J=1,JMAX
 JMMJ=JMAX-J+1
  WRITE(6,47)  (V(I,JMMJ),I=1,IMAX)
7002  CONTINUE
 IF(SWRL.NE.1) GO TO 7014
  WRITE(6,52)
  DO 7003 J=1,JMAX
 JMMJ=JMAX-J+1
  WRITE(6,47)  (W(I,JMMJ),I=1,IMAX)
7003  CONTINUE
7014     CONTINUE
  WRITE(6,51)
  DO 7004 J=1, JMAX
 JMMJ=JMAX-J+1
  WRITE(6,47)  (P(I,JMMJ),I=1,IMAX)
7004  CONTINUE
47    FORMAT(12(,E11.4))
48     FORMAT(//,2X,8H U-FIELD,/)
49     FORMAT(///,2X,8H V-FIELD,/)
```

```
51     FORMAT(///,2X,8H P-FIELD,/)
52     FORMAT(///,2X,8H W-FIELD,/)
53     FORMAT(6X,5HITER=,I5,9X,5HTIME=,1PE12.5,10X,6HCYCLE=,I4)
       RETURN
       END
       SUBROUTINE PLOT (U,V,IMAX,JMAX)
C      ===============================================================
C      S U B R O U T I N E   P L O T   G R A P H E S   T H E   U , V   V E -
C      L O C I T Y   C O M P O N E N T S   I N   V E C T O R I A L   F O R M
C      ===============================================================
       DIMENSION V(15,30),U(15,30),VJ(15,30),UJ(15,30)
       WRITE(60,25)
 25    FORMAT(10X,*PLTL*)
       JM1=JMAX-1
       IM1=IMAX-1
C-------------------------------------------------------------------
       DO 1 J=2,JM1
       DO  1 I=2,IM1
       VJ(I,J)=(V(I,J)+V(I,J-1))/2*100
       UJ(I,J)=(U(I,J)+U(I-1,J))/2*100
 1     CONTINUE
       NEWDELX=10000/IM1-20
       NEWDELY=10000/JM1-20
C-------------------------------------------------------------------
       DO  731 I=1,IM1
       DO  731  J=1,JM1
       INCRY=(J-1)*NEWDELY
       INCRX=(I-1)*NEWDELX
       WRITE(60,105) INCRX,INCRY
 105   FORMAT(5X,I4,5X,I4,*^ *)
       IVELX=INCRX+UJ(I,J)
       IVELY=INCRY+VJ(I,J)
       WRITE (60,106) IVELX,IVELY
 106   FORMAT(5X,I4,5X,I4)
 731   CONTINUE
       WRITE(60,26)
 26    FORMAT(10X,*PLTT*)
       RETURN
       END
```